PLANNER-R1: REWARD SHAPING ENABLES EFFICIENT AGENTIC RL WITH SMALLER LLMS

Anonymous authors
Paper under double-blind review

ABSTRACT

We investigated Agentic RL with large language models on the TRAVELPLANNER benchmark. Our approach, PLANNER-R1, achieved a **56.9%** final-pass rate with only 180 training queries, a $2.7\times$ improvement over GPT-5's 21.2% baseline and the strongest agentic result on the public leaderboard. A central finding was that smaller models (8B) were highly responsive to reward shaping: with dense process-level signals, they reached competitive performance while being $3.5\times$ more compute-efficient and $1.5\times$ more memory-efficient than 32B models. Larger models were more robust under sparse rewards but exhibited smaller relative gains from shaping and higher variance across runs. While curriculum learning offered no significant benefit, shaped rewards consistently amplified learning dynamics, making 8B models the most efficient setting for agentic RL. Crucially, these gains did not come at the cost of overfitting: fine-tuned models mostly maintained or exceeded baseline performance on out-of-domain tasks, including MULTI-IF, NATURALPLAN, and τ-BENCH. These results establish reward shaping as a decisive lever for scaling agentic RL, highlight the competitive strength of smaller models, and demonstrate that efficiency can be achieved without sacrificing generalization.

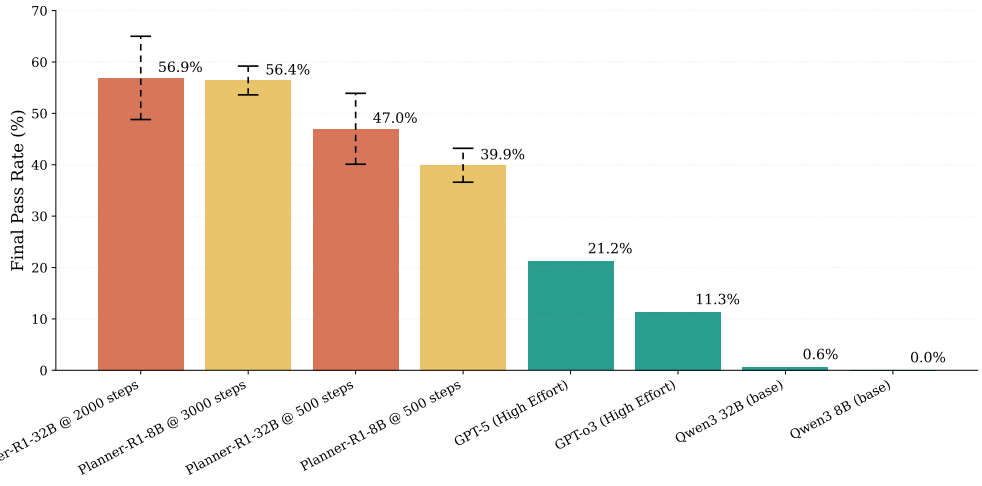

Figure 1: Final-pass rate on the leaderboard test set for tool-use travel planning. Our Planner-R1 models outperformed SOTA LLMs reaching 56.9% average final pass rate.

1 INTRODUCTION

Large Language Models (LLMs) have recently posted striking gains in deliberate reasoning and decision making, propelled in part by large-scale reinforcement learning (RL) that trains models to *think before they answer* (OpenAI et al., 2024a; Guo et al., 2025). Beyond language understanding, LLM agents now demonstrate emerging competence in structured reasoning, tool use, and multi-step problem solving across embodied and web environments (Wang et al., 2023a; Huang et al.,

2024; Feng et al., 2025). Yet turning these abilities into *reliable* long-horizon execution under real-world constraints remains challenging: prompting-only agents such as ReAct and Reflexion frequently mis-sequence actions, loop, or hallucinate when tasks demand coordinated tool use and strict constraint satisfaction (Yao et al., 2023b; Shinn et al., 2023).

Planning tasks such as meeting scheduling and multi-day itineraries are demanding: agents must coordinate *heterogeneous tools* (calendars, maps, flights, booking APIs), satisfy *hard, interdependent constraints*, and maintain *global consistency* over long horizons. TRAVELPLANNER makes these difficulties concrete by casting travel itinerary creation as tool-augmented, constraint-driven planning (Xie et al., 2024). The benchmark provides a sandbox with nearly four million records and $1{,}225$ curated intents with reference plans, and evaluates whether an agent can gather evidence via tools and synthesize itineraries that satisfy both explicit user constraints and commonsense feasibility. At release, even strong models struggled—e.g., GPT-4-Turbo with ReAct achieved only a 0.6% *final pass rate* on the $1{,}000$-example test split—underscoring the gap between fluent language modeling and dependable constraint-aware planning (Xie et al., 2024).

To close this gap, researchers have explored different training paradigms. A natural starting point is behavior cloning via supervised fine-tuning (SFT), where a teacher generates "golden" trajectories and a policy maximizes their likelihood, often masking environment observations and tool outputs. While simple and widely used, SFT largely imitates expert behavior and is brittle under distribution shift or suboptimal data. This motivates the search for approaches that directly optimize for end-task success rather than imitation fidelity. RL provides precisely such a mechanism: rewards encode task success, and the policy is updated to increase the likelihood of action sequences that satisfy constraints while suppressing those that fail. Recent work has shown that RL can deliver state-of-the-art gains in model-based reasoning and planning (OpenAI et al., 2024a; Guo et al., 2025), making it a promising direction for tackling long-horizon tool use in TRAVELPLANNER. In addition to model performance, there is growing interest in building efficient agentic systems with smaller models (Belcak et al., 2025). Such models show promising potential for inference and training efficiency, but there remains limited understanding of how agentic RL can best improve their performance without overfitting. Our study addresses this gap by examining how model size, reward shaping, and efficiency interact in agentic RL.

We formulate TRAVELPLANNER as a multi-step, tool-use MDP with constraint-aware planning, where the agent gathers missing facts, reconciles conflicts, and outputs a structured itinerary. Training uses agentic RL with trajectory-level rewards gated by schema validity. Our main focus is the role of *reward density*: we vary feedback from dense, process-level signals to sparse final-pass rewards, and also test a curriculum that transitions between them. All reward variants are *properly shaped*, ensuring they converge to the same optimal policy while revealing how granularity influences learning dynamics. Our contributions are summarized below.

- **SOTA Tool-Use on TravelPlanner** PLANNER-R1-32B achieved a $\mathbf{56.9}\%$ final-pass rate on the official 1,000-query test split, a $2.7\times$ improvement over GPT-5. This is the strongest agentic result on TRAVELPLANNER, demonstrating that RL-tuned models can surpass state-of-the-art proprietary models.[1]
- **Reward shaping dynamics** We find a strong link between reward granularity and policy competence. Smaller models (8B) were especially responsive to shaped, process-level rewards, achieving performance competitive with 32B models while being up to $3.5\times$ more compute-efficient and $1.5\times$ more memory-efficient. Larger models (32B) performed well across reward settings and remained more robust under sparse signals, but exhibited higher variance. In contrast, 8B models depended more heavily on dense shaping. Curriculum learning alone provided no measurable benefit, whereas reward shaping consistently amplified learning dynamics, making the 8B models the most efficient setting for agentic RL.
- **Generalization Beyond Training Domain** Our agents did not overfit to TRAVELPLANNER: Planner-R1 models mostly maintained or exceeded baseline performance on out-of-domain tasks including MULTI-IF, NATURALPLAN, and τ-BENCH. This demonstrates that the efficiency gains from agentic RL come without sacrificing robustness, supporting transfer to diverse planning and tool-use settings.

[1] Hao et al. (2025) achieved 93.9% correctness with external SAT/SMT solvers; our focus is on end-to-end agentic planning without such solvers.

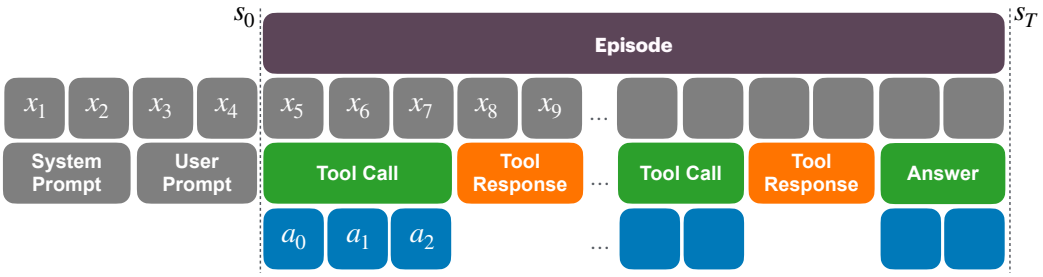

Figure 2: MDP Visualization. x_i represent the ith token, while a_t represents the action the agent took at time t. Notice that initial prompts and tool responses contain tokens, but they dont increase the time step t.

- **RL Benchmark Formulation** We recast TRAVELPLANNER as a multi-step agentic RL benchmark by leveraging the official sandbox and its seven tools, and we designed verifiable reward functions aligned with the task's success criteria. Policies were trained with VERL(ver, 2024), where our system-level optimizations reduced runtime and memory usage by 20%, enabling efficient large-scale experimentation. (see Appendix A for details)

2 PLANNER RL

2.1 PROBLEM FORMULATION

We cast tool-augmented planning as a Markov Decision Process (MDP) $\mathcal{M} = (\mathcal{S}, \mathcal{A}, P, r, \gamma)$. Since our MDP is episodic, we set $\gamma = 1$. Each episode is initialized with two textual inputs: a *system prompt* y, which defines the agent's role and available tools (see Appendix B.1), and a *user prompt* u, which specifies the task goal and user preferences. At each time step t, the agent interacts with the environment by emitting a token, alternating between natural language and structured tool invocations, until it decides that a complete plan has been formed. Figure 2 illustrates this process. While our instantiation focuses on the TRAVELPLANNER benchmark (Xie et al., 2024), the formulation is general and extends naturally to other agentic RL tasks. We next describe the individual components of the MDP:

States. $s_t \in \mathcal{S}$ denotes the complete history, including the initial system and user prompt, the agent's partial plan, and all tool calls and responses observed up to step t, beginning from $s_0 = (y, u)$.

Actions. $a_t \in \mathcal{A}$ is the generated token at time t. The agent issues *tool calls* through tokens to gather the necessary information and then produces the final plan through a *text action*. Tool calls are realized as seven APIs connected to a sandbox with millions of grounded records: `search_flights`, `search_accommodations`, `search_restaurants`, `search_attractions`, `search_ground_transportation`, `get_cities`, and `calculator`. Each call takes JSON arguments and is wrapped inside `<tool_call>...</tool_call>`, returning a structured JSON object: successful calls yield a list of serialized rows, while failures return an error field.

Compared to the original TRAVELPLANNER, we added the `calculator` API for explicit numeric reasoning and disabled the lightweight semantic memory so that tool responses appear directly in the context. The final text action directly outputs an itinerary enclosed in `<answer>...</answer>`. This design standardizes iterative tool use while keeping the final deliverable unambiguous.

Transitions. The environment appends each action to the state; if a tool call is completed, it is executed and the output o_t is added, otherwise o_t is null. The next state is $s_{t+1} = (s_t, a_t, o_{t+1})$, with older context truncated when exceeding the window. A key difference from the original benchmark (Xie et al., 2024) is that we append tokens chronologically to the state, making our transition more generic, as opposed to moving the tool responses to a specific part of the context.

Reward. In this domain, success is sparse and binary. A plan receives a reward of one only at termination if it is schema-valid and satisfies both commonsense and user-specified constraints. User queries are designed to ensure that at least one feasible plan exists.

To pass schema validation, the plan must be a valid *JSON array of day-level objects*, each conforming to a fixed schema with fields for `days`, `city`, `transportation`, `attraction`, `accommodation`, `breakfast`, `lunch`, `dinner`. Importantly, `city` and `transportation` are typed objects with required fields (e.g., transportation must specify mode, origin, destination, and duration), rather than free-form strings. The full schema is provided in Appendix B.2.

Constraints fall into two categories. First, there are N_{cs} *commonsense constraints*, which are not explicitly given to the agent but must nonetheless be satisfied (e.g., transportation segments cannot overlap). Second, there are N_{hard} *hard constraints*, explicitly specified in the user prompt, such as departure and return dates. Formal definitions and the complete list of constraints are provided in the work of Xie et al. (2024).

Our objective is to learn a policy $\pi_\theta(a \mid s)$ that maximizes the expected cumulative reward, which here reduces to optimizing the terminal reward: $\max_\theta \ \mathbb{E}_{\pi_\theta}[r_T]$.

2.2 Multi-Stage Reward

Due to the extreme sparsity of the reward function, we shape it using auxiliary metrics defined in the original paper. In particular,

- $r_{\text{schema}} = \mathbb{I}[\text{plan conforms to schema}]$: indicator of schema compliance,
- $r_{\text{cs}}^{\text{micro}} = \frac{S_{\text{cs}}}{N_{\text{cs}}}$: fraction of satisfied commonsense constraints,
- $r_{\text{hard}}^{\text{micro}} = \frac{S_{\text{hard}}}{N_{\text{hard}}}$: fraction of satisfied hard constraints,
- $r_{\text{cs}}^{\text{macro}} = \mathbb{I}\big[r_{\text{cs}}^{\text{micro}} = 1\big]$: indicator that all commonsense constraints pass,
- $r_{\text{hard}}^{\text{macro}} = \mathbb{I}\big[r_{\text{hard}}^{\text{micro}} = 1\big]$: indicator that all hard constraints pass,
- $r_{\text{pass}} = \mathbb{I}[r_{\text{cs}}^{\text{macro}} \wedge r_{\text{hard}}^{\text{macro}}]$: indicator that both commonsense and hard constraints pass.

Here, $\mathbb{I}$ is the indicator function. The micro rewards are necessary to provide partial credit when all constraints are not met , the macro rewards emphasize satisfying entire categories, and r_{pass} corresponds to the original evaluation metric. The terminal reward in the generic form can then be written as:

$$r = r_{\text{schema}}\Big(\lambda_1 r_{\text{cs}}^{\text{micro}} + \lambda_2 r_{\text{hard}}^{\text{micro}} + \lambda_3 r_{\text{cs}}^{\text{macro}} + \lambda_4 r_{\text{hard}}^{\text{macro}} + \lambda_5 r_{\text{pass}}\Big). \tag{1}$$

By adjusting $\lambda = [\lambda_1, \ldots, \lambda_5]$, we control the reward density. In practice, we consider three stages:

- Stage 1: $\lambda = [1, 1, 1, 1, 1]$ (dense feedback),
- Stage 2: $\lambda = [0, 0, 1, 1, 1]$ (category-level),
- Stage 3: $\lambda = [0, 0, 0, 0, 1]$ (sparse final pass).

This setup defines proper reward shaping: auxiliary terms provide intermediate guidance, while the final-pass reward captures the true objective. Crucially, all of the above weightings preserve the same optimal policy. Building on this, we define a curriculum that schedules λ across training, beginning with dense feedback for partial credit, then shifting to category-level rewards, and finally collapsing to the sparse end reward. Transitions occur at predefined step counts.

2.3 Optimization

We used GRPO (Shao et al., 2024), a clipped PPO-style objective without KL regularization. For each planning query $u \in \mathcal{D}$, we sample G trajectories $\mathcal{T} = \{\tau_i\}_{i=1}^{G}$ with corresponding Returns $\mathbf{r} = \{r_1, r_2, \cdots, r_G\}$ from the behavior policy $\pi_{\theta_{\text{old}}}$, where $\tau_i = (s_0^i, a_0^i, \ldots, s_{T_i}^i)$. The loss is

$$\mathcal{J}_{\text{GRPO}}(\theta) = \mathbb{E}_{u\sim\mathcal{D},\,\{\tau_i\}\sim\pi_{\theta_{\text{old}}}}\left[\frac{1}{G}\sum_{i=1}^{G}\frac{1}{T_i}\sum_{t=0}^{T_i-1}\min\Big(\rho_\theta^{i,t}\,\hat{A}_i,\ \text{clip}(\rho_\theta^{i,t},\,1-\epsilon,\,1+\epsilon)\,\hat{A}_i\Big)\right], \tag{2}$$

with clipping hyperparameter $\epsilon > 0$. The token-level importance ratio and trajectory-level advantage are defined as

$$\rho_\theta^{i,t} = \frac{\pi_\theta(a_t^i \mid s_t^i, a_{<t}^i)}{\pi_{\theta_{\text{old}}}(a_t^i \mid s_t^i, a_{<t}^i)}, \qquad \hat{A}_i = \frac{r_i - \text{mean}(\mathbf{r})}{\text{std}(\mathbf{r})}.$$

3 EMPIRICAL RESULTS

3.1 SETUP

In-Domain We fine-tuned Qwen3 8B/32B models across 5 runs with fixed set of seeds on TRAVELPLANNER. Due to GPU memory and context budget constraints, and inspired by the recent findings that thinking may not always improve performance (Gema et al., 2025; Shojaee* et al., 2025), we did not enable "thinking-in-context." We named these models Planner-R1. The official 45/180 train–validation split was merged and reshuffled into 180 training and 45 validation queries, while preserving the easy/medium/hard ratio. We evaluated three single-stage reward configurations with 500 steps and a curriculum regime for 8B and 32B models with 100/300/100 and 50/350/100 steps respectively.[2] 8 rollouts were executed in `sglang` with a standard ReAct-style agent. We capped trajectories at 30 steps, tool responses at 8,192 tokens, and model outputs at 30,500 tokens. All runs used two nodes (16×H200 GPUs). We used learning rate of 10^{-6}. Although Qwen3 provided an explicit `<think>...</think>` mode (qwe, 2025b;a), the additional reasoning tokens inflated context length and, in pilots, yielded no gains on task metrics. Full hyperparameters and implementation details are given in Appendix B.3, and decoding and sampling presets are summarized in Appendix B.4.

Out-of-Domain A central concern with task-specific fine-tuning is whether it harms generalization outside the target domain. To probe this, we evaluated our trained models on three complementary suites. All were unseen during training, with evaluation limited to task instructions. (i) NATURAL PLAN (Zheng et al., 2024) (Trip Planning, Meeting Planning, Calendar Scheduling), where tool outputs were provided as context and accuracy was scored by *Exact Match*; we followed the official five-shot prompting protocol. (ii) MULTI-IF (He et al., 2024) (English), a multi-turn instruction-following benchmark derived from IFEval, where the input at turn t concatenated all prior turns ($\leq t-1$); we reported the mean of turn-wise scores. (iii) τ-BENCH (Yao et al., 2024) (retail, function-calling), which measured goal completion against a simulated backend and policy documents; we reported pass@1.

3.2 EVALUATIONS

Table 1 depicts the TRAVELPLANNER results based on Qwen3 (Yang et al., 2025), GPT (OpenAI et al., 2024b; OpenAI, 2025b;a), and our Planner-R1 models using four reward models across five metrics defined in 2. Numbers after $\pm$ indicates 95% confidence intervals.

Base models showed partial competence but struggled with full constraint satisfaction. While stronger base models achieved 99%+ delivery rates and moderate commonsense and hard-constraint coverage, they did not perform well end-to-end. For instance, GPT-5 and GPT-o3 achieved final pass rates of 21.2% and 11.3%, respectively. In contrast, the open-weight Qwen3 series performed substantially worse: the 8B model failed entirely, and the 32B model achieved only 0.6% final pass despite a 41.9% delivery rate. This stark disparity underscored that the challenge lay not in planning individual items, but in coordinating tool calls and enforcing all constraints jointly. Prior work (Yao et al., 2023b; Nakano et al., 2021) suggested that prompting alone often underutilized tool feedback, whereas robustness emerged when models interleaved reasoning with actions to query, observe, and update plans. Our findings, as we will see in Section 4, align with this view: base models were able to generate fluent itineraries, but their failures centered on tool sequencing and constraint bookkeeping rather than basic retrieval.

Agentic RL delivered large gains; smaller models were reward-sensitive. RL fine tuning improved both 8B and 32B Qwen3 substantially. Specifically PLANNER-R1-8B using Stage 1 reward and PLANNER-R1-32B using Curriculum reward reached 39.9% and 47% final pass rates respectively. Compared to the 32B model, the 8B model was more sensitive towards sparser rewards: using Stage 2 and Stage 3 rewards resulted in $3/5$ and $5/5$ model collapses respectively, showing the importance of reward shaping (Ng et al., 1999; dos Santos et al., 2024; Qian et al., 2025b). These collapses explain the large confidence intervals of Stage 2 results. 32B models were more robust. All

[2]Given the strong Stage 3 performance of larger models, we advanced them more quickly from Stage 1.

reward resulted in 42%+ final pass rate, although increased sparsity resulted in increased variance. 32B model learnt best with Curriculum reward yet the difference were not statistically significant.

Smaller models delivered superior GPU efficiency compared to larger ones. Given the strong performance of Stage 1 training, we extended experiments with high-capacity settings, training the 8B model for 3,000 steps and the 32B model for 2,000 steps. Figure 3 reports results from five independent runs. The left panel, plotted against training steps, shows that both models achieved broadly similar performance trajectories. The right panel, however, plots final pass rate against estimated FLOPs (see Appendix B.6 for details) and reveals a clear efficiency gap. While the 32B model reached 90% of its peak performance (52.3%) at 7.6×10^{20} FLOPs, the 8B model achieved the same level at only 2.1×10^{20} FLOPs, a $3.5\times$ improvement in efficiency. Although 32B models attained a slightly higher peak accuracy (56.9% vs. 56.4%), this difference was not statistically significant and came with higher variance. A complementary *memory-efficiency* analysis appears in Appendix B.5, where we discuss GPU memory footprint and its implications for agentic RL with long multi-turn contexts. Overall, the FLOPs-based comparison highlights that smaller models are substantially more GPU-efficient for agentic RL training using shaped rewards when data generation is not a limiting factor.

Table 1: Results on the TRAVELPLANNER test set. For Planner-R1 models, we report mean performance with 95% confidence intervals over five runs at 500 training steps. Stage 1–3 denote runs trained exclusively on one stage for 500 steps each. Curriculum uses three phases: for 8B, 100/300/100 steps; for 32B, 50/350/100 steps across Stages 1–3.

Method	**Delivery Rate (%)**	**Commonsense**		**Hard Constraint**		**Final Pass Rate (%)**
		Micro (%)	**Macro (%)**	**Micro (%)**	**Macro (%)**	
Qwen3-8B	0.0	0.0	0.0	0.0	0.0	0.0
Qwen3-32B	41.9	27.5	1.7	11.4	7.2	0.6
GPT-o3 (high)	99.6	74.2	14.3	57.7	48.0	11.3
GPT5 (high)	99.8	81.0	23.4	75.4	71.1	21.2
Planner-R1-8B						
Stage1	99.5±0.8	94.8±1.2	69.0±6.9	61.0±2.6	46.2±2.5	39.9±4.3
Stage2	99.9±0.2	80.6±18.2	30.2±51.9	63.4±13.8	48.6±16.3	13.3±23.2
Stage3	0.0±0.0	0.0±0.0	0.0±0.0	0.0±0.0	0.0±0.0	0.0±0.0
Curriculum	99.7±0.8	92.7±3.1	57.9±18.6	53.9±5.7	38.2±4.2	27.1±12.6
Planner-R1-32B						
Stage1	99.3±1.6	95.2±1.6	70.4±13.4	74.2±1.4	56.4±2.9	42.3±8.0
Stage2	91.1±0.5	87.7±2.2	69.1±14.5	70.0±5.6	55.0±7.6	44.1±9.4
Stage3	99.4±0.9	94.7±2.5	71.9±15.2	60.8±16.6	48.2±15.1	44.3±14.1
Curriculum	99.1±1.7	95.9±2.5	78.5±7.9	72.1±5.0	55.1±6.2	47.0±6.9

RL fine-tuned models generalized beyond the training domain. Table 2 shows that RL fine-tuned models performed mostly on par with, and often surpassed, their pretrained counterparts across NATURAL PLAN (Zheng et al., 2024), MULTI-IF (He et al., 2024), and τ-BENCH (Yao et al., 2024). Blue and red indicate significant improvements and degradations, respectively. After 2,000 steps, both models improved on most metrics, and even at 3,000 steps the 8B model outperformed baselines on five of seven metrics with marginal regressions on two metrics. We attribute this robustness to the JSON-gated output structure, which couples semantics with format and reinforces tool-conditioned behaviors, consistent with prior findings that structured generation improves reliability (Oestreich et al., 2025) and supports generalization to unseen schemas (Liu et al., 2019).

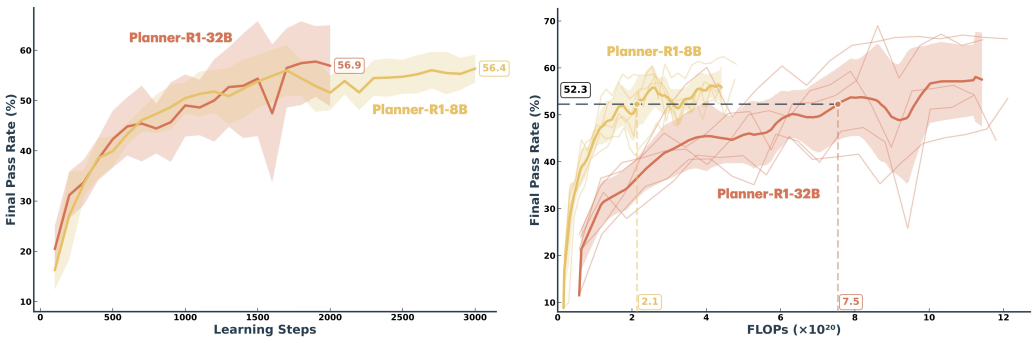

Figure 3: Performance of 8B and 32B Planner-R1 during training based on learning steps (left) and training FLOPS (right). The horizontal dashed line highlights 90% of the maximum average performance of 32B models, while vertical dashed lines show the required FLOPs to reach that performance by both 8B and 32B models.

Table 2: Transferability to external benchmarks without target-domain training (percent). Models are evaluated on NATURAL PLAN, MULTI-IF, and τ-BENCH. Blue = significant improvement over the base model; red = significant degradation from the base model.

Method (Training Steps)	**NATURAL PLAN**			**Multi-IF**			**τ-bench**
	Trip	Meeting	Calendar	1st-Turn	2nd-Turn	3rd-Turn	Pass@1
Qwen3-8B	12.9±0.2	82.0±0.0	22.7±0.3	88.9±0.6	82.8±0.6	75.4±0.5	9.5±2.1
Planner-R1-8B (500)	14.0±0.9	83.2±1.1	24.3±0.9	89.4±0.4	83.5±0.7	76.9±0.6	11.1±0.9
Planner-R1-8B (2000)	14.0±2.1	84.0±0.6	23.2±2.1	89.8±0.4	84.0±0.5	77.2±0.4	12.1±2.3
Planner-R1-8B (3000)	10.7±1.8	84.5±1.3	20.1±2.0	89.8±0.1	83.9±0.4	76.7±0.4	15.1±3.1
Qwen3-32B	11.3±0.0	77.0±0.0	32.2±0.0	89.1±0.3	83.1±0.3	77.1±0.4	28.0±2.2
Planner-R1-32B (500)	15.7±2.2	79.8±1.6	33.2±0.5	88.7±0.2	83.4±0.6	77.7±0.6	28.7±2.1
Planner-R1-32B (2000)	19.5±1.2	80.2±1.1	34.4±1.4	89.8±0.3	84.1±0.3	78.5±0.4	33.9±3.8

4 QUALITATIVE ANALYSIS

To illustrate the effects of RL and model scale, we present a qualitative analysis of Planner-R1 8B and 32B models across training checkpoints, with GPT-5 included as a reference point. We highlight progression in failure modes, tool use, and subreward acquisition for the trained models, and report failure patterns for GPT-5.

Failure Progression Figure 4 shows the progression of the top five failure categories for Planner-R1 8B (left) and 32B (right) models during training[3]. For hallucination detection, we verify whether the origin city, destination city, attractions, accommodations, and restaurants are present in the corresponding databases. Both models began with high failure rates, particularly on accommodation and cost constraints. For the 8B model, hallucination and cost remain persistent challenges, while all other failures fall below 10% after 800 steps. For the 32B model, accommodation and cost remain dominant errors, with all other failures dropping below 10% by 600 steps. Notably, the 32B model exhibits substantially fewer hallucinations but struggles more with finding accommodations that qualify, for example when the chosen accommodation has a minimum-night requirement and the planned stay must meet this constraint. Another stark observation is the spike at 1,600 steps which can be also observed in Figure 3. In general, we found 32B models with more variations, specially in one run the pass rate dropped from 44% to 26% to 51% impacting the average.

Tool-Use Progression We observed clear improvements in tool-use behavior as training progressed. Early checkpoints of both the 8B and 32B models exhibited poor sequencing, often looping on

[3]Top categories selected based on their AUC during training. For another lens with top 3 failures at each learning step see Figure A.2

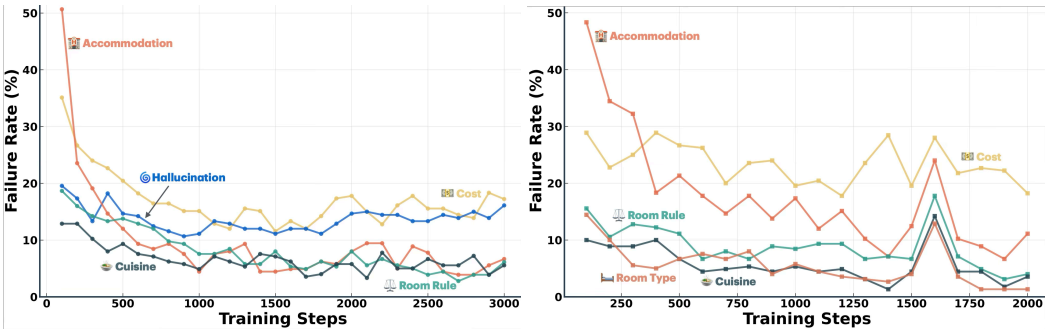

Figure 4: Progression of top 5 failures for 8B (left) and 32B (right) Planner-R1 during training

repetitive calls (e.g., repeatedly invoking the calculator or restaurant tools), which led to incoherent or incomplete plans. As training progressed, both model failures shifted from syntactic to semantic failures: they returned schema valid plans but often failed to call necessary tools to meet the required constraints. With more training, models could often return valid plans. For further details, see the visualizations of tool-call trajectories in Appendix Figures A.3-A.12.

Sub-Reward Progression For both 8B and 32B models, the initial ranking of subrewards from highest to lowest was consistent (see Figure A.1 in Appendix): (1) Schema, (2) Commonsense Micro, (3) Hard Micro, (4) Commonsense Macro, (5) Hard Macro, and (6) Final Pass. As training progressed, success rates increased across all categories, yet this relative ordering remained largely unchanged. This pattern aligned with the λ values defined in Section 2.2, reinforcing our intuition about the relative difficulty of these subrewards and underscoring the role of reward shaping in guiding models through progressively harder objectives.

GPT-5 Behavior Across multiple scenarios, GPT-5 exhibits several recurring error patterns. These include repetition errors, such as selecting the same restaurant or revisiting a city multiple times in violation of commonsense constraints; incomplete plans, where the model fails to return to the departing city or omits key itinerary elements; constraint violations, such as booking fewer than the required minimum hotel nights; and hallucinations, including inventing non-existent hotels or skipping required meals. Illustrative examples of these failure modes are provided in Appendix A.4–A.8.

5 Related Work

Planning Early *chain-of-thought* prompting showed that writing out intermediate steps boosts LLM performance on complex QA and math (Wei et al., 2022; Kojima et al., 2022). Subsequent variants—most notably self-consistency and structured schemes such as *Least-to-Most* and *Plan-and-Solve*—further reduce errors by decomposing problems and aggregating diverse solution paths (Wang et al., 2023c; Zhou et al., 2023; Wang et al., 2023b). To address the brittleness of linear chains, *search-based* methods recast reasoning as combinatorial exploration with lookahead and backtracking, operating over trees (*Tree of Thoughts*) and graphs (*Graph of Thoughts*) (Yao et al., 2023a; Besta et al., 2024). Multi-agent formulations extend this idea via division of labor: *Chain-of-Agents* partitions long inputs among workers while a manager aggregates their outputs (Chen et al., 2024). Decoupling planning from execution further improves robustness: *Plan-and-Act* pairs a planner with an executor and scales supervision via synthetic trajectories, while *Iterative Programmatic Planning* treats planning as code synthesis (Erdogan et al., 2025; Aravindan et al., 2025). Formal methods offer another angle: Hao et al. (2025) translate planning queries into SAT/SMT specifications solved by external verifiers, achieving rigorous correctness guarantees; in contrast, we keep planning internal to the agent and optimize policies end-to-end with RL. Finally, to reach beyond the context window, recent systems interleave reasoning with targeted search: *Search-o1* triggers agentic retrieval under uncertainty and distills evidence via a Reason-in-Documents step, while *AI-SearchPlanner* trains a lightweight RL planner to trade off query utility and cost, yielding cross-model gains (Li et al., 2025a; Mei et al., 2025).

Agentic RL RL is increasingly used to make tool-use strategic and long-horizon: *Search–R1* learns to issue multi-turn web queries during reasoning (Jin et al., 2025), *SkyRL* trains multi-turn agents inside real software environments (Cao et al., 2025), and *ReTool* interleaves Python execution within the reasoning loop under outcome-based rewards (Feng et al., 2025). Complementing these, the Tool-Integrated Reasoning line embeds tools directly into the RL objective: *ToRL* scales tool-integrated RL from base models and reports emergent selective tool invocation with strong math gains (Li et al., 2025b), while *ToolRL* systematically studies reward design for tool selection and parameterization, showing that carefully shaped rewards with GRPO yield robust improvements over SFT (Qian et al., 2025a). *Biomni* applies end-to-end reinforcement learning, creating rewards and RL environments tailored to biomedicine, scalably training the agent to carry out research tasks more effectively (Huang et al., 2025). In parallel, large-scale RL fine-tuning (*Kimi k1.5*, *DeepSeek–R1*) boosts general reasoning, and *Qwen3* introduces dynamic "thinking" vs. "non-thinking" modes to balance depth and latency (Kimi Team et al., 2025; Guo et al., 2025; Yang et al., 2025). Building on this momentum, *Kimi K2* emphasizes open agentic intelligence with agentic data synthesis and a joint RL stage (Kimi Team, 2025); *GLM-4.5* proposes ARC (Agentic, Reasoning, Coding) foundation models with hybrid thinking/direct modes and RL post-training (GLM-4.5 Team, 2025); and Microsoft's *rStar2–Agent* explores reliable Python tool use with a Resample-on-Correct strategy for agentic RL (Shang et al., 2025). Most closely related, Chen et al. (2025) introduce LOOP, a data- and memory-efficient variant of PPO that enables reinforcement learning for interactive digital agents directly within stateful, multi-domain environments such as AppWorld.

Discussion and Limitations

We showed that agentic RL can substantially enhance planning with tool use, using TravelPlanner as a testbed. Our method achieved state-of-the-art performance among open-weight models and outperformed GPT-5 baselines by **2.7×**. A key finding is that smaller models (8B) are especially responsive to shaped, process-level rewards: with only 180 training queries, they reached competitive performance with 32B models while operating at up to **3.5× higher compute-efficiency** and **1.5x higher memory-efficiency**. Larger models were more robust under sparse signals but gained less from shaping and exhibited greater variability and higher compute demand, underscoring reward design as a key lever for scaling efficiency.

These efficiency gains at $2{,}000$ steps did not come at the expense of robustness. Fine-tuned models maintained or exceeded baseline performance on out-of-domain benchmarks such as Multi-IF, NaturalPlan, and τ-Bench, showing no evidence of overfitting. At $3{,}000$ steps, the 8B model still improved 5 of 7 metrics but regressed on 2, highlighting a potential drawback of excessive fine-tuning. Although our study followed leaderboard rules and avoided prompt engineering, both baselines and our method may benefit from future prompt optimization.

Our study also has limitations. We focus on TravelPlanner, a constrained benchmark, and smaller models may not remain competitive on more complex or open-ended tasks. While 8B models are more FLOP-efficient, larger models can reach higher peak accuracy, which may be necessary in applications where absolute performance is critical. Finally, we explored curriculum learning only in a simple staged form, leaving richer scheduling strategies for future work. Overall, our results highlight reward shaping as central to agentic RL and position smaller models as an efficient, generalizable path forward.

References

verl: Volcano engine reinforcement learning for llms. https://github.com/volcengine/verl, 2024. Open-source implementation of the HybridFlow paper.

Qwen3-8b: Switching between thinking and non-thinking mode. https://huggingface.co/Qwen/Qwen3-8B#switching-between-thinking-and-non-thinking-mode, 2025a. Accessed: 2025-09-24.

Qwen3: Think deeper, act faster. https://qwenlm.github.io/blog/qwen3/, 2025b. Accessed: 2025-09-24.

Ashwath Vaithinathan Aravindan, Zhisheng Tang, and Mayank Kejriwal. Code-driven planning in grid worlds with large language models. *arXiv preprint arXiv:2505.10749*, 2025.

Peter Belcak, Greg Heinrich, Shizhe Diao, Yonggan Fu, Xin Dong, Saurav Muralidharan, Yingyan Celine Lin, and Pavlo Molchanov. Small language models are the future of agentic ai, 2025. URL https://arxiv.org/abs/2506.02153.

Maciej Besta, Nils Blach, Ales Kubicek, Robert Gerstenberger, Michał Podstawski, Lukas Gianinazzi, Joanna Gajda, Tomasz Lehmann, Hubert Niewiadomski, Piotr Nyczyk, et al. Graph of thoughts: solving elaborate problems with large language models. In *Proceedings of the Thirty-Eighth AAAI Conference on Artificial Intelligence and Thirty-Sixth Conference on Innovative Applications of Artificial Intelligence and Fourteenth Symposium on Educational Advances in Artificial Intelligence*, pp. 17682–17690, 2024.

Shiyi Cao, Sumanth Hegde, Dacheng Li, Tyler Griggs, Shu Liu, Eric Tang, Jiayi Pan, Xingyao Wang, et al. Skyrl-v0: Train real-world long-horizon agents via reinforcement learning, 2025. arXiv:2502.02789.

Kevin Chen, Marco Cusumano-Towner, Brody Huval, Aleksei Petrenko, Jackson Hamburger, Vladlen Koltun, and Philipp Krähenbühl. Reinforcement learning for long-horizon interactive llm agents. *arXiv preprint arXiv:2502.01600*, 2025. URL https://arxiv.org/abs/2502.01600.

Tianjun Chen et al. Chain of agents: Toward long context reasoning in language models via multi-agent cooperation. *arXiv preprint arXiv:2406.02818*, 2024.

Joao dos Santos et al. Revisiting sparse rewards for goal-reaching reinforcement learning. *arXiv:2407.00324*, 2024. URL https://arxiv.org/abs/2407.00324.

Lutfi Eren Erdogan, Nicholas Lee, Sehoon Kim, Suhong Moon, Hiroki Furuta, Gopala Anumanchipalli, Kurt Keutzer, and Amir Gholami. Plan-and-act: Improving planning of agents for long-horizon tasks. *arXiv preprint arXiv:2503.09572*, 2025.

Jiazhan Feng, Shijue Huang, Xingwei Qu, Ge Zhang, et al. Retool: Reinforcement learning for strategic tool use in llms. *arXiv preprint arXiv:2504.11536*, 2025.

Aryo Pradipta Gema, Alexander Hägele, Runjin Chen, Andy Arditi, Jacob Goldman-Wetzler, Kit Fraser-Taliente, Henry Sleight, Linda Petrini, Julian Michael, Beatrice Alex, Pasquale Minervini, Yanda Chen, Joe Benton, and Ethan Perez. Inverse scaling in test-time compute, 2025. URL https://arxiv.org/abs/2507.14417.

GLM-4.5 Team. Glm-4.5: Agentic, reasoning, and coding (arc) foundation models, 2025.

Daya Guo, Dejian Yang, Haowei Zhang, Junxiao Song, Peiyi Wang, Qihao Zhu, Runxin Xu, Ruoyu Zhang, Shirong Ma, Xiao Bi, et al. Deepseek-r1 incentivizes reasoning in llms through reinforcement learning. *Nature*, 645(8081):633–638, 2025.

Yilun Hao, Yongchao Chen, Yang Zhang, and Chuchu Fan. Large language models can solve real-world planning rigorously with formal verification tools, 2025. URL https://arxiv.org/abs/2404.11891.

Yun He, Di Jin, Chaoqi Wang, Chloe Bi, Karishma Mandyam, Hejia Zhang, Chen Zhu, Ning Li, Tengyu Xu, Hongjiang Lv, et al. Multi-if: Benchmarking llms on multi-turn and multilingual instructions following. *arXiv preprint arXiv:2410.15553*, 2024.

Kexin Huang, Serena Zhang, Hanchen Wang, Yuanhao Qu, Yingzhou Lu, Yusuf Roohani, Ryan Li, Lin Qiu, Gavin Li, Junze Zhang, Di Yin, Shruti Marwaha, Jennefer N. Carter, Xin Zhou, Matthew Wheeler, Jonathan A. Bernstein, Mengdi Wang, Peng He, Jingtian Zhou, Michael Snyder, Le Cong, Aviv Regev, and Jure Leskovec. Biomni: A general-purpose biomedical ai agent. *bioRxiv*, 2025. doi: 10.1101/2025.05.30.656746. URL https://www.biorxiv.org/content/early/2025/06/02/2025.05.30.656746.

Xu Huang, Weiwen Liu, Xiaolong Chen, Xingmei Wang, Hao Wang, Defu Lian, Yasheng Wang, Ruiming Tang, and Enhong Chen. Understanding the planning of llm agents: A survey, 2024. URL https://arxiv.org/abs/2402.02716.

Bowen Jin, Hansi Zeng, Zhenrui Yue, Jinsung Yoon, Sercan O. Arik, Dong Wang, Hamed Zamani, and Jiawei Han. Search-r1: Training llms to reason and leverage search engines with reinforcement learning. *arXiv preprint arXiv:2503.09516*, 2025.

Kimi Team. Kimi k2: Open agentic intelligence, 2025.

Kimi Team, Angang Du, Bofei Gao, Bowei Xing, et al. Kimi k1.5: Scaling reinforcement learning with large language models. *arXiv preprint arXiv:2501.12599*, 2025.

Takeshi Kojima, Shixiang Shane Gu, Machel Reid, Yutaka Matsuo, and Yusuke Iwasawa. Large language models are zero-shot reasoners. In *Advances in Neural Information Processing Systems (NeurIPS)*, pp. 22199–22213, 2022.

Xiaoxi Li, Guanting Dong, Jiajie Jin, Yuyao Zhang, Yujia Zhou, Yutao Zhu, Peitian Zhang, and Zhicheng Dou. Search-o1: Agentic search-enhanced large reasoning models. *arXiv preprint arXiv:2501.05366*, 2025a.

Xuefeng Li, Haoyang Zou, and Pengfei Liu. Torl: Scaling tool-integrated rl. *arXiv preprint arXiv:2503.23383*, March 2025b. doi: 10.48550/arXiv.2503.23383. URL https://arxiv.org/abs/2503.23383.

Tianyu Liu, Furu Wei, and Ming Zhou Wang. Table-to-text generation with unseen schemas. In *Proceedings of the 57th Annual Meeting of the Association for Computational Linguistics*, 2019.

Lang Mei, Zhihan Yang, and Chong Chen. Ai-searchplanner: Modular agentic search via pareto-optimal multi-objective reinforcement learning. *arXiv preprint arXiv:2508.20368*, 2025.

Reiichiro Nakano et al. Webgpt: Browser-assisted question-answering with human feedback. *arXiv:2112.09332*, 2021. URL https://arxiv.org/abs/2112.09332.

Andrew Y. Ng, Daishi Harada, and Stuart Russell. Policy invariance under reward transformations: Theory and application to reward shaping. In *ICML*, pp. 278–287, 1999. URL https://people.eecs.berkeley.edu/~pabbeel/cs287-fa09/readings/NgHaradaRussell-shaping-ICML1999.pdf.

Julian Oestreich, Lydia Müller, et al. Evaluating structured decoding for text-to-table generation: Evidence from three datasets. *arXiv preprint arXiv:2508.15910*, 2025.

OpenAI. Gpt-5 system card. https://cdn.openai.com/gpt-5-system-card.pdf, 2025a. Accessed: 2025-09-20.

OpenAI. Openai o3 and o4-mini system card. https://cdn.openai.com/pdf/2221c875-02dc-4789-800b-e7758f3722c1/o3-and-o4-mini-system-card.pdf, 2025b. Accessed: 2025-09-20.

OpenAI, :, Aaron Jaech, Adam Kalai, Adam Lerer, Adam Richardson, Ahmed El-Kishky, Aiden Low, Alec Helyar, Aleksander Madry, Alex Beutel, Alex Carney, Alex Iftimie, Alex Karpenko, Alex Tachard Passos, Alexander Neitz, Alexander Prokofiev, Alexander Wei, Allison Tam, Ally Bennett, Ananya Kumar, Andre Saraiva, Andrea Vallone, Andrew Duberstein, Andrew Kondrich, Andrey Mishchenko, Andy Applebaum, Angela Jiang, Ashvin Nair, Barret Zoph, Behrooz Ghorbani, Ben Rossen, Benjamin Sokolowsky, Boaz Barak, Bob McGrew, Borys Minaiev, Botao Hao, Bowen Baker, Brandon Houghton, Brandon McKinzie, Brydon Eastman, Camillo Lugaresi, Cary Bassin, Cary Hudson, Chak Ming Li, Charles de Bourcy, Chelsea Voss, Chen Shen, Chong Zhang, Chris Koch, Chris Orsinger, Christopher Hesse, Claudia Fischer, Clive Chan, Dan Roberts, Daniel Kappler, Daniel Levy, Daniel Selsam, David Dohan, David Farhi, David Mely, David Robinson, Dimitris Tsipras, Doug Li, Dragos Oprica, Eben Freeman, Eddie Zhang, Edmund Wong, Elizabeth Proehl, Enoch Cheung, Eric Mitchell, Eric Wallace, Erik Ritter, Evan Mays, Fan Wang, Felipe Petroski Such, Filippo Raso, Florencia Leoni, Foivos Tsimpourlas, Francis Song, Fred von Lohmann, Freddie Sulit, Geoff Salmon, Giambattista Parascandolo, Gildas Chabot, Grace Zhao, Greg Brockman, Guillaume Leclerc, Hadi Salman, Haiming Bao, Hao Sheng, Hart Andrin, Hessam Bagherinezhad, Hongyu Ren, Hunter Lightman, Hyung Won Chung, Ian Kivlichan, Ian O'Connell, Ian Osband, Ignasi Clavera Gilaberte, Ilge Akkaya, Ilya Kostrikov, Ilya Sutskever, Irina Kofman, Jakub Pachocki, James Lennon, Jason Wei, Jean Harb, Jerry Twore, Jiacheng Feng,

Jiahui Yu, Jiayi Weng, Jie Tang, Jieqi Yu, Joaquin Quiñonero Candela, Joe Palermo, Joel Parish, Johannes Heidecke, John Hallman, John Rizzo, Jonathan Gordon, Jonathan Uesato, Jonathan Ward, Joost Huizinga, Julie Wang, Kai Chen, Kai Xiao, Karan Singhal, Karina Nguyen, Karl Cobbe, Katy Shi, Kayla Wood, Kendra Rimbach, Keren Gu-Lemberg, Kevin Liu, Kevin Lu, Kevin Stone, Kevin Yu, Lama Ahmad, Lauren Yang, Leo Liu, Leon Maksin, Leyton Ho, Liam Fedus, Lilian Weng, Linden Li, Lindsay McCallum, Lindsey Held, Lorenz Kuhn, Lukas Kondraciuk, Lukasz Kaiser, Luke Metz, Madelaine Boyd, Maja Trebacz, Manas Joglekar, Mark Chen, Marko Tintor, Mason Meyer, Matt Jones, Matt Kaufer, Max Schwarzer, Meghan Shah, Mehmet Yatbaz, Melody Y. Guan, Mengyuan Xu, Mengyuan Yan, Mia Glaese, Mianna Chen, Michael Lampe, Michael Malek, Michele Wang, Michelle Fradin, Mike McClay, Mikhail Pavlov, Miles Wang, Mingxuan Wang, Mira Murati, Mo Bavarian, Mostafa Rohaninejad, Nat McAleese, Neil Chowdhury, Neil Chowdhury, Nick Ryder, Nikolas Tezak, Noam Brown, Ofir Nachum, Oleg Boiko, Oleg Murk, Olivia Watkins, Patrick Chao, Paul Ashbourne, Pavel Izmailov, Peter Zhokhov, Rachel Dias, Rahul Arora, Randall Lin, Rapha Gontijo Lopes, Raz Gaon, Reah Miyara, Reimar Leike, Renny Hwang, Rhythm Garg, Robin Brown, Roshan James, Rui Shu, Ryan Cheu, Ryan Greene, Saachi Jain, Sam Altman, Sam Toizer, Sam Toyer, Samuel Miserendino, Sandhini Agarwal, Santiago Hernandez, Sasha Baker, Scott McKinney, Scottie Yan, Shengjia Zhao, Shengli Hu, Shibani Santurkar, Shraman Ray Chaudhuri, Shuyuan Zhang, Siyuan Fu, Spencer Papay, Steph Lin, Suchir Balaji, Suvansh Sanjeev, Szymon Sidor, Tal Broda, Aidan Clark, Tao Wang, Taylor Gordon, Ted Sanders, Tejal Patwardhan, Thibault Sottiaux, Thomas Degry, Thomas Dimson, Tianhao Zheng, Timur Garipov, Tom Stasi, Trapit Bansal, Trevor Creech, Troy Peterson, Tyna Eloundou, Valerie Qi, Vineet Kosaraju, Vinnie Monaco, Vitchyr Pong, Vlad Fomenko, Weiyi Zheng, Wenda Zhou, Wes McCabe, Wojciech Zaremba, Yann Dubois, Yinghai Lu, Yining Chen, Young Cha, Yu Bai, Yuchen He, Yuchen Zhang, Yunyun Wang, Zheng Shao, and Zhuohan Li. Openai o1 system card, 2024a. URL https://arxiv.org/abs/2412.16720.

OpenAI, Josh Achiam, Steven Adler, Sandhini Agarwal, Lama Ahmad, Ilge Akkaya, Florencia Leoni Aleman, Diogo Almeida, Janko Altenschmidt, Sam Altman, Shyamal Anadkat, Red Avila, Igor Babuschkin, Suchir Balaji, Valerie Balcom, Paul Baltescu, Haiming Bao, Mohammad Bavarian, Jeff Belgum, Irwan Bello, Jake Berdine, Gabriel Bernadett-Shapiro, Christopher Berner, Lenny Bogdonoff, Oleg Boiko, Madelaine Boyd, Anna-Luisa Brakman, Greg Brockman, Tim Brooks, Miles Brundage, Kevin Button, Trevor Cai, Rosie Campbell, Andrew Cann, Brittany Carey, Chelsea Carlson, Rory Carmichael, Brooke Chan, Che Chang, Fotis Chantzis, Derek Chen, Sully Chen, Ruby Chen, Jason Chen, Mark Chen, Ben Chess, Chester Cho, Casey Chu, Hyung Won Chung, Dave Cummings, Jeremiah Currier, Yunxing Dai, Cory Decareaux, Thomas Degry, Noah Deutsch, Damien Deville, Arka Dhar, David Dohan, Steve Dowling, Sheila Dunning, Adrien Ecoffet, Atty Eleti, Tyna Eloundou, David Farhi, Liam Fedus, Niko Felix, Simón Posada Fishman, Juston Forte, Isabella Fulford, Leo Gao, Elie Georges, Christian Gibson, Vik Goel, Tarun Gogineni, Gabriel Goh, Rapha Gontijo-Lopes, Jonathan Gordon, Morgan Grafstein, Scott Gray, Ryan Greene, Joshua Gross, Shixiang Shane Gu, Yufei Guo, Chris Hallacy, Jesse Han, Jeff Harris, Yuchen He, Mike Heaton, Johannes Heidecke, Chris Hesse, Alan Hickey, Wade Hickey, Peter Hoeschele, Brandon Houghton, Kenny Hsu, Shengli Hu, Xin Hu, Joost Huizinga, Shantanu Jain, Shawn Jain, Joanne Jang, Angela Jiang, Roger Jiang, Haozhun Jin, Denny Jin, Shino Jomoto, Billie Jonn, Heewoo Jun, Tomer Kaftan, Łukasz Kaiser, Ali Kamali, Ingmar Kanitscheider, Nitish Shirish Keskar, Tabarak Khan, Logan Kilpatrick, Jong Wook Kim, Christina Kim, Yongjik Kim, Jan Hendrik Kirchner, Jamie Kiros, Matt Knight, Daniel Kokotajlo, Łukasz Kondraciuk, Andrew Kondrich, Aris Konstantinidis, Kyle Kosic, Gretchen Krueger, Vishal Kuo, Michael Lampe, Ikai Lan, Teddy Lee, Jan Leike, Jade Leung, Daniel Levy, Chak Ming Li, Rachel Lim, Molly Lin, Stephanie Lin, Mateusz Litwin, Theresa Lopez, Ryan Lowe, Patricia Lue, Anna Makanju, Kim Malfacini, Sam Manning, Todor Markov, Yaniv Markovski, Bianca Martin, Katie Mayer, Andrew Mayne, Bob McGrew, Scott Mayer McKinney, Christine McLeavey, Paul McMillan, Jake McNeil, David Medina, Aalok Mehta, Jacob Menick, Luke Metz, Andrey Mishchenko, Pamela Mishkin, Vinnie Monaco, Evan Morikawa, Daniel Mossing, Tong Mu, Mira Murati, Oleg Murk, David Mély, Ashvin Nair, Reiichiro Nakano, Rajeev Nayak, Arvind Neelakantan, Richard Ngo, Hyeonwoo Noh, Long Ouyang, Cullen O'Keefe, Jakub Pachocki, Alex Paino, Joe Palermo, Ashley Pantuliano, Giambattista Parascandolo, Joel Parish, Emy Parparita, Alex Passos, Mikhail Pavlov, Andrew Peng, Adam Perelman, Filipe de Avila Belbute Peres, Michael Petrov, Henrique Ponde de Oliveira Pinto, Michael, Pokorny, Michelle Pokrass, Vitchyr H. Pong, Tolly Powell, Alethea Power, Boris Power, Elizabeth Proehl,

Raul Puri, Alec Radford, Jack Rae, Aditya Ramesh, Cameron Raymond, Francis Real, Kendra Rimbach, Carl Ross, Bob Rotsted, Henri Roussez, Nick Ryder, Mario Saltarelli, Ted Sanders, Shibani Santurkar, Girish Sastry, Heather Schmidt, David Schnurr, John Schulman, Daniel Selsam, Kyla Sheppard, Toki Sherbakov, Jessica Shieh, Sarah Shoker, Pranav Shyam, Szymon Sidor, Eric Sigler, Maddie Simens, Jordan Sitkin, Katarina Slama, Ian Sohl, Benjamin Sokolowsky, Yang Song, Natalie Staudacher, Felipe Petroski Such, Natalie Summers, Ilya Sutskever, Jie Tang, Nikolas Tezak, Madeleine B. Thompson, Phil Tillet, Amin Tootoonchian, Elizabeth Tseng, Preston Tuggle, Nick Turley, Jerry Tworek, Juan Felipe Cerón Uribe, Andrea Vallone, Arun Vijayvergiya, Chelsea Voss, Carroll Wainwright, Justin Jay Wang, Alvin Wang, Ben Wang, Jonathan Ward, Jason Wei, CJ Weinmann, Akila Welihinda, Peter Welinder, Jiayi Weng, Lilian Weng, Matt Wiethoff, Dave Willner, Clemens Winter, Samuel Wolrich, Hannah Wong, Lauren Workman, Sherwin Wu, Jeff Wu, Michael Wu, Kai Xiao, Tao Xu, Sarah Yoo, Kevin Yu, Qiming Yuan, Wojciech Zaremba, Rowan Zellers, Chong Zhang, Marvin Zhang, Shengjia Zhao, Tianhao Zheng, Juntang Zhuang, William Zhuk, and Barret Zoph. Gpt-4 technical report, 2024b. URL https://arxiv.org/abs/2303.08774.

Cheng Qian, Emre Can Acikgoz, Qi He, Hongru Wang, Xiusi Chen, Dilek Hakkani-Tür, Gokhan Tur, and Heng Ji. Toolrl: Reward is all tool learning needs. *arXiv preprint arXiv:2504.13958*, April 2025a. doi: 10.48550/arXiv.2504.13958. URL https://arxiv.org/abs/2504.13958.

Cheng Qian, Emre Can Acikgoz, Qi He, Hongru Wang, Xiusi Chen, Dilek Hakkani-Tür, Gokhan Tür, and Heng Ji. Toolrl: Reward is all tool learning needs. *arXiv:2504.13958*, 2025b. URL https://arxiv.org/abs/2504.13958.

Ning Shang, Yifei Liu, Yi Zhu, Li Lyna Zhang, Weijiang Xu, Xinyu Guan, Buze Zhang, Bingcheng Dong, Xudong Zhou, Bowen Zhang, Ying Xin, Ziming Miao, Scarlett Li, Fan Yang, and Mao Yang. rstar2-agent: Agentic reasoning technical report, 2025. Microsoft Research.

Zhihong Shao, Peiyi Wang, Qihao Zhu, Runxin Xu, Junxiao Song, Xiao Bi, Haowei Zhang, Mingchuan Zhang, Y. K. Li, Y. Wu, and Daya Guo. Deepseekmath: Pushing the limits of mathematical reasoning in open language models, 2024. URL https://arxiv.org/abs/2402.03300.

Noel Shinn, Federico Cassano, Ashwin Gopinath, Karthik R. Narasimhan, and Shunyu Yao. Reflexion: Language agents with verbal reinforcement learning. In *Advances in Neural Information Processing Systems (NeurIPS)*, 2023.

Parshin Shojaee*, Iman Mirzadeh*, Keivan Alizadeh, Maxwell Horton, Samy Bengio, and Mehrdad Farajtabar. The illusion of thinking: Understanding the strengths and limitations of reasoning models via the lens of problem complexity, 2025. URL https://ml-site.cdn-apple.com/papers/the-illusion-of-thinking.pdf.

Guanhua Wang, Yuzhuo Xie, Yuanzhi Jiang, Ajay Mandlekar, Chongjie Xiao, Yuke Zhu, Lifeng Fan, and Anima Anandkumar. Voyager: An open-ended embodied agent with large language models. *arXiv preprint arXiv:2305.16291*, 2023a.

Lei Wang, Wanyu Xu, Yihuai Lan, Zhiqiang Hu, Yunshi Lan, Roy Ka-Wei Lee, and Ee-Peng Lim. Plan-and-solve prompting: Improving zero-shot chain-of-thought reasoning by large language models. In *Annual Meeting of the Association for Computational Linguistics (ACL)*, pp. 2609–2634, 2023b.

Xuezhi Wang, Jason Wei, Dale Schuurmans, Quoc V. Le, Ed H. Chi, Sharan Narang, Aakanksha Chowdhery, and Denny Zhou. Self-consistency improves chain of thought reasoning in language models. In *International Conference on Learning Representations (ICLR)*, 2023c.

Jason Wei, Xuezhi Wang, Dale Schuurmans, Maarten Bosma, Ed H. Chi, Quoc V. Le, and Denny Zhou. Chain-of-thought prompting elicits reasoning in large language models. In *Advances in Neural Information Processing Systems (NeurIPS)*, pp. 24824–24837, 2022.

Jian Xie, Kai Zhang, Jiangjie Chen, Tinghui Zhu, Renze Lou, Yuandong Tian, Yanghua Xiao, and Yu Su. Travelplanner: a benchmark for real-world planning with language agents. In *Proceedings of the 41st International Conference on Machine Learning*, pp. 54590–54613, 2024.

An Yang, Anfeng Li, Baosong Yang, Beichen Zhang, Binyuan Hui, Bo Zheng, Bowen Yu, Chang Gao, Chengen Huang, Chenxu Lv, Chujie Zheng, Dayiheng Liu, Fan Zhou, Fei Huang, Feng Hu, Hao Ge, Haoran Wei, Huan Lin, Jialong Tang, Jian Yang, Jianhong Tu, Jianwei Zhang, Jianxin Yang, Jiaxi Yang, Jing Zhou, Jingren Zhou, Junyang Lin, Kai Dang, Keqin Bao, Kexin Yang, Le Yu, Lianghao Deng, Mei Li, Mingfeng Xue, Mingze Li, Pei Zhang, Peng Wang, Qin Zhu, Rui Men, Ruize Gao, Shixuan Liu, Shuang Luo, Tianhao Li, Tianyi Tang, Wenbiao Yin, Xingzhang Ren, Xinyu Wang, Xinyu Zhang, Xuancheng Ren, Yang Fan, Yang Su, Yichang Zhang, Yinger Zhang, Yu Wan, Yuqiong Liu, Zekun Wang, Zeyu Cui, Zhenru Zhang, Zhipeng Zhou, and Zihan Qiu. Qwen3 technical report. *arXiv preprint arXiv:2505.09388*, 2025. https://arxiv.org/abs/2505.09388.

Shunyu Yao, Dian Yu, Jeffrey Zhao, Izhak Shafran, Thomas L. Griffiths, Yuan Cao, and Karthik Narasimhan. Tree of thoughts: Deliberate problem solving with large language models. In *Advances in Neural Information Processing Systems (NeurIPS)*, 2023a.

Shunyu Yao, Jeffrey Zhao, Dian Yu, Nan Du, Izhak Shafran, Karthik R. Narasimhan, and Yuan Cao. React: Synergizing reasoning and acting in language models. In *International Conference on Learning Representations (ICLR)*, 2023b.

Shunyu Yao, Noah Shinn, Pedram Razavi, and Karthik Narasimhan. τ-Bench: A Benchmark for Tool–Agent–User Interaction in Real-World Domains. *arXiv preprint arXiv:2406.12045*, 2024.

Huaixiu Steven Zheng, Swaroop Mishra, Hugh Zhang, Xinyun Chen, Minmin Chen, Azade Nova, Le Hou, Heng-Tze Cheng, Quoc V Le, Ed H Chi, et al. Natural plan: Benchmarking llms on natural language planning. *arXiv preprint arXiv:2406.04520*, 2024.

Denny Zhou, Nathanael Schärli, Le Hou, Jason Wei, Nathan Scales, Xuezhi Wang, Dale Schuurmans, Claire Cui, Olivier Bousquet, Quoc V. Le, and Ed H. Chi. Least-to-most prompting enables complex reasoning in large language models. In *International Conference on Learning Representations (ICLR)*, 2023.

A System-Level Optimizations

Overview. RL training with large-scale LLMs requires co-locating both training and inference engines on the same set of GPUs. This dual demand creates severe memory pressure, often leading to out-of-memory (OOM) errors when switching between training and rollout phases. To address this, we integrated memory management techniques into our RL Pipelines.

Multi-Stage Awake Memory Management. In VERL, reinforcement learning (RL) training is conducted in Colocate Mode, where both the training engine (e.g., FSDP) and inference engine (e.g., SGLang) share the same GPU resources. A major bottleneck arises when transferring weights from the training engine to the inference engine: model parameters must be copied from FSDP into SGLang, often causing out-of-memory (OOM) failures under high memory pressure.

To address this, we extended the *Sleep/Awake* mechanism in SGLang and introduced the *Multi-Stage Awake* strategy for fine-grained memory management during rollouts. Instead of a single monolithic resume, memory resumption is divided into multiple stages:

1. Load training model weights into GPU memory.
2. Resume inference model weights at preserved virtual addresses.
3. Synchronize weights between training and rollout engines.
4. Offload training model weights back to CPU.
5. Resume the KV cache region for rollout execution.

This staged approach minimizes memory waste and prevents fragmentation. Our empirical results show that it provides two key benefits:

- **Enables training of larger models**: With the same KV cache ratio, our approach reduces peak GPU memory by **20–23%**, which unblocks stable training of a 32B-parameter model on 8×H200 GPUs even at higher cache ratios (0.8, 0.85, and up to 0.9). Without Multi-Stage Awake, training consistently ran out of memory beyond 0.7.
- **Improves throughput**: For the same model size, our method allows a larger KV cache ratio to be used, directly improving inference throughput. While throughput gains are workload-dependent and not easily comparable across setups, our experiments show that increasing the ratio from 0.7 to 0.9 leads to significant improvements in rollout efficiency.

B Implementation Details

B.1 System Prompt

We include the jinja template of our full system prompt used for Planner-R1 during training/evaluation.

```
You are a helpful travel assistant that plans detailed travel
↪  itineraries by calling external functions (tools). You have access
↪  to the following tools and must use them as needed to gather
↪  accurate, up-to-date information.

# Behavior Guidelines
- If a task requires multiple steps or tools, proceed step by step,
↪  calling ONE TOOL per turn.
- Never assume details-always verify all information using tools.
- When you have gathered sufficient information to finalize the plan,
↪  respond with an <answer> block with the final itinerary in valid
↪  JSON format.

# Tool Usage Rules
- Do not repeat the same tool call with identical arguments.
- Always provide complete and correct function arguments.

# Final Plan Format
Once all necessary information is collected, respond with the final
↪  plan:
```
<answer>
  [
    {
      // Day 1 plan following schema
    },
    {
      // Day 2 plan following schema
    },
    // ... additional days
  ]
</answer>
```
**IMPORTANT CONSTRAINTS**
- The <answer> must contain ONLY valid JSON, strictly following the
↪  plan_schema.
- Do not include any explanatory text inside the <answer> block.
- Do not output <answer> until all needed tool calls are completed.

# Final Plan Schema
Each element in the <answer> JSON array should represent a single day
↪  of the trip and follow this schema exactly:
```json
```
```

```
{{ plan_schema }}
```

B.2 PLAN JSON SCHEMA

The final itinerary must be a JSON *array* of per-day objects. Each day object is validated against the schema below. This structured contract doubles as a checklist (ensuring coverage of all required fields) and enables automatic reward gating.

```
{
    "type": "object",
    "required": [
        "days", "city", "transportation", "attraction",
        ↪ "accommodation", "breakfast", "lunch", "dinner"
    ],
    "properties": {
        "days": {
            "description": "The day number of the plan starting from
            ↪ 1.",
            "type": "integer"
        },
        "city": {
            "description": "Can be a city name string if no transfer
            ↪ is needed, or an dict with 'from' and 'to' keys that
            ↪ indicates the origin and destination city.",
            "oneOf": [
                {"type": "string"},
                {
                    "type": "object",
                    "required": ["from", "to"],
                    "properties": {
                        "from": {"type": "string"},
                        "to": {"type": "string"}
                    },
                    "additionalProperties": false
                }
            ]
        },
        "transportation": {
            "description": "Either '-' if no transportation is needed,
            ↪ or an object describing the transportation details.
            ↪ Instead of total cost, use per person price for flight
            ↪ and per vehicle cost for taxi/self-driving as the
            ↪ cost.",
            "oneOf": [
                {
                    "type": "string",
                    "const": "-"
                },
                {
                    "type": "object",
                    "required": ["mode", "from", "to", "duration",
                    ↪ "distance", "cost"],
                    "properties": {
                        "mode": {
                            "type": "string",
                            "enum": ["flight", "taxi",
                            ↪ "self-driving"],
                            "description": "Type of transportation."
                        },
```

```
                        "from": {"type": "string", "description":
                        ↪  "Origin city"},
                        "to": {"type": "string", "description":
                        ↪  "Destination city"},
                        "duration": {"type": "string", "description":
                        ↪  "Transportation duration"},
                        "distance": {"type": "string", "description":
                        ↪  "Distance of the trip"},
                        "cost": {"type": "integer", "description":
                        ↪  "Cost of the transportation"},

                        "flight_number": {"type": "string",
                        ↪  "description": "Flight number (for flights
                        ↪  only)"},
                        "departure_time": {"type": "string",
                        ↪  "description": "Flight departure time"},
                        "arrival_time": {"type": "string",
                        ↪  "description": "Flight arrival time"}
                    },
                    "additionalProperties": false
                }
            ]
        },
        "attraction": {
            "description": "A list of attraction names planned for the
            ↪  day, or '-' if no attractions are planned.",
            "oneOf": [
                {"type": "string", "const": "-"},
                {
                    "type": "array",
                    "items": {"type": "string"},
                    "minItems": 1
                }
            ]
        },
        "accommodation": {
            "description": "The name of the accommodation for today.
            ↪  '-' if no accommodation is needed.",
            "type": "string"
        },
        "breakfast": {
            "description": "The name of the breakfast restaurant for
            ↪  today. '-' if no breakfast is planned.",
            "type": "string"
        },
        "lunch": {
            "description": "The name of the lunch restaurant for
            ↪  today. '-' if no lunch is planned.",
            "type": "string"
        },
        "dinner": {
            "description": "The name of the dinner restaurant for
            ↪  today. '-' if no dinner is planned.",
            "type": "string"
        }
    },
    "additionalProperties": false
}
```

B.3 Training, Validation, and Evaluation Setup

RL framework and resources. We train with VERL using **GRPO** on **2 nodes** with **8 GPUs/node** (16 H200 GPUs total). Rollouts use **sglang** with a multi-turn, tool-augmented agent (ReAct-style).

Training configuration. Stage 1/2/3 share the same VERL configuration; only the reward weights differ by stage (see Sec. 2). File paths are pseudonymized for readability.

```yaml
# verl + GRPO. Stage-agnostic; change reward weights per stage.
actor_rollout_ref:
  actor:
    strategy: fsdp
    ppo_mini_batch_size: 8
    ppo_micro_batch_size: null
    ppo_micro_batch_size_per_gpu: 1
    use_dynamic_bsz: false
    ppo_max_token_len_per_gpu: 16384
    clip_ratio: 0.2
    clip_ratio_low: 0.2
    clip_ratio_high: 0.2
    policy_loss:
      loss_mode: vanilla
      clip_cov_ratio: 0.0002
      clip_cov_lb: 1.0
      clip_cov_ub: 5.0
      kl_cov_ratio: 0.0002
      ppo_kl_coef: 0.1
    clip_ratio_c: 3.0
    loss_agg_mode: token-mean
    entropy_coeff: 0
    use_kl_loss: false
    use_torch_compile: true
    kl_loss_coef: 0.001
    kl_loss_type: low_var_kl
    ppo_epochs: 1
    shuffle: false
    optim:
      lr: 1.0e-06
      lr_warmup_steps_ratio: 0.0
      total_training_steps: -1
      weight_decay: 0.01
      lr_warmup_steps: -1
      min_lr_ratio: 0.0
      num_cycles: 0.5
      warmup_style: constant
    grad_clip: 1.0
    ulysses_sequence_parallel_size: 1
    entropy_from_logits_with_chunking: false
    entropy_checkpointing: false
    fsdp_config:
      wrap_policy:
        min_num_params: 0
      param_offload: true
      optimizer_offload: true
      offload_policy: false
      reshard_after_forward: true
      fsdp_size: -1
      forward_prefetch: false
  rollout:
    name: sglang
    mode: async
    temperature: 1.0
    top_k: -1
```

```yaml
    top_p: 1
    prompt_length: 2268
    response_length: 30500
    dtype: bfloat16
    gpu_memory_utilization: 0.6
    ignore_eos: false
    enforce_eager: true
    free_cache_engine: true
    tensor_model_parallel_size: 4
    max_num_batched_tokens: 8192
    max_model_len: null
    max_num_seqs: 1024
    log_prob_micro_batch_size: null
    log_prob_micro_batch_size_per_gpu: 32
    log_prob_use_dynamic_bsz: false
    log_prob_max_token_len_per_gpu: 16384
    disable_log_stats: true
    do_sample: true
    n: 8
    multi_stage_wake_up: false
    val_kwargs:
      top_k: -1
      top_p: 1.0
      temperature: 0
      n: 1
      do_sample: false
    multi_turn:
      enable: true
      max_assistant_turns: 30
      tool_config_path: ${PROJ_ROOT}/config/tool_config.yaml
      max_user_turns: 30
      max_parallel_calls: 1
      max_tool_response_length: 8192
      tool_response_truncate_side: right
      interaction_config_path: null
      completion_callback: null
      use_inference_chat_template: false
      tokenization_sanity_check_mode: strict
      format: hermes
    calculate_log_probs: false
    agent:
      num_workers: 8
      agent_loop_config_path: ${PROJ_ROOT}/config/agent_loops.yaml
      custom_async_server:
        path: null
        name: null
    update_weights_bucket_megabytes: 512
    enable_chunked_prefill: true
    load_format: dummy_dtensor
    layered_summon: false
    enable_thinking: false
  hybrid_engine: true
  model:
    path: Qwen/Qwen3-{8B|32B}  # base model
    custom_chat_template: null
    use_shm: false
    external_lib: null
    override_config: {}
    enable_gradient_checkpointing: true
    enable_activation_offload: false
    use_remove_padding: true
    target_modules: all-linear
    exclude_modules: null
    use_liger: false
```

```yaml
    use_fused_kernels: false
    fused_kernel_options:
      impl_backend: torch
    trust_remote_code: false
trainer:
  balance_batch: true
  total_epochs: 300
  total_training_steps: 3000
  profile_steps: null
  logger:
    - mlflow
  log_val_generations: 0
  rollout_data_dir: null
  nnodes: 2
  n_gpus_per_node: 8
  save_freq: 100
  esi_redundant_time: 0
  resume_mode: auto
  val_before_train: true
  val_only: false
  test_freq: 50
  critic_warmup: 0
  default_hdfs_dir: null
  del_local_ckpt_after_load: false
  max_actor_ckpt_to_keep: null
  max_critic_ckpt_to_keep: null
  ray_wait_register_center_timeout: 300
  device: cuda
  use_legacy_worker_impl: auto
data:
  tokenizer: null
  use_shm: false
  train_files: ${PROJ_ROOT}/data/train.parquet
  val_files: ${PROJ_ROOT}/data/test.parquet
  prompt_key: prompt
  reward_fn_key: data_source
  max_prompt_length: 2268
  max_response_length: 30500
  train_batch_size: 16
  val_batch_size: 64
  return_raw_input_ids: false
  return_raw_chat: true
  return_full_prompt: false
  shuffle: true
  dataloader_num_workers: 8
  validation_shuffle: false
  filter_overlong_prompts: true
  filter_overlong_prompts_workers: 1
  truncation: error
  image_key: images
  video_key: videos
  trust_remote_code: false
custom_reward_function:
  path: ${PROJ_ROOT}/rewards_v3.py
  name: compute_score
algorithm:
  gamma: 1.0
  lam: 1.0
  adv_estimator: grpo
  norm_adv_by_std_in_grpo: true
  use_kl_in_reward: false
  kl_penalty: kl
  kl_ctrl:
    type: fixed
```

```
    kl_coef: 0.001
    horizon: 10000
    target_kl: 0.1
  use_pf_ppo: false
  pf_ppo:
    reweight_method: pow
    weight_pow: 2.0
```

Listing 1: VERL/GRPO configuration (paths pseudonymized). Stage 2/3 reuse this config with stage-specific reward weights.

Evaluation protocol. We evaluate on the TRAVELPLANNER *official test set* by reusing the VERL *validation* pipeline to keep decoding/sampling consistent with validation:

1. Point the VERL validation loader to the official test split (same sampler settings as validation).
2. Run validation to **dump trajectories** locally (tool calls, responses, final answers) as JSONL.
3. **Post-process** each final answer: validate against the plan schema (App. B.2), enforce JSON-gated output, and **convert** to the leaderboard's submission format.
4. **Upload** the converted file to the TRAVELPLANNER leaderboard; report Delivery, micro/macro commonsense, micro/macro hard, and Final.

B.4 DECODING AND SAMPLING SETTINGS

We standardize decoding across training and evaluation to isolate the effect of learning. Table 3 summarizes the presets we use for different contexts; "Common runtime limits" apply to all scenarios unless noted. For Validation/Test we reuse VERL's validation path on the official TP test split (Sec. B.3).

Common runtime limits.

- **Max response tokens:** 30,500 (`response_length`)
- **Max tool response tokens:** 8,192 (`max_tool_response_length`)
- **Agent turns cap:** 30 assistant turns; 30 tool turns
- **Tool-call cap:** 30 calls

Table 3: Decoding presets by context.

Context	do_sample	Temp	Top-p	Top-k	n
Training	true	1.0	1.0	-1	8
Validation / Test	false	0.0	1.0	-1	1
NaturalPlan	true	1.0	1.0	-1	1
Multi-IF	false	0.7	0.8	20	1
τ-bench	false	0.6	0.95	20	1

B.5 GPU MEMORY FOOTPRINT AND PRACTICAL EFFICIENCY

In the same 2-node/16-GPU training setup, PLANNER-R1-8B uses approximately $\sim$60 GB of GPU memory per device, whereas PLANNER-R1-32B requires $\geq$90 GB per device. This difference has practical consequences: the 8B configuration runs comfortably on H100s, while the 32B configuration necessitates higher-memory accelerators (e.g., H200). The gap is especially relevant for agentic RL, where multi-turn interactions and tool feedback produce long contexts and large key–value (KV) caches during rollouts, amplifying the memory pressure beyond the update phase.

B.6 ESTIMATING TRAINING FLOPS FROM VERL'S MFU

MFU in VERL (what it is). VERL reports a *model FLOPs utilization* (MFU): the fraction of the cluster's "promised" peak compute achieved during *policy updates*. Internally it is computed per

update as

$$\text{MFU} = \frac{f_{\text{ach}}\, E}{f_{\text{peak}}\, W}, \qquad f_{\text{ach}} = \frac{\text{FLOPs}_{\text{update}}}{t_{\text{actor}}},$$

where E is the number of GRPO epochs per batch, W is the number of GPUs (world size), f_{peak} is the *promised FLOPs rate per GPU* used by VERL in its MFU denominator, t_{actor} is the time spent in the parameter-update step, and $\text{FLOPs}_{\text{update}}$ is the per-step FLOPs consumed by that update. The in-tree FLOPs counter aggregates *forward + backward* over all layers/tokens.

Reconstruction used in this paper. Solving for $\text{FLOPs}_{\text{update}}$ gives

$$\boxed{\text{FLOPs}_{\text{update}} = \text{MFU} \times f_{\text{peak}} \times W \times \frac{t_{\text{actor}}}{E}}$$

In our runs $E{=}1$ and $W{=}16$. We set $f_{\text{peak}}{=}\,9.89 \times 10^{14}$ FLOPs/s per GPU—the same constant VERL uses for MFU—so the reconstruction matches its calculation.

Practical proxy for t_{actor}. VERL does not log t_{actor} each step, but it logs `update_policy_time` (t_{policy}), which equals the actor update plus brief offload/reload bookkeeping. Because the parameter update dominates, we use

$$t_{\text{actor}} \approx t_{\text{policy}} \quad \Rightarrow \quad \text{FLOPs}_{\text{update}} \approx \text{MFU} \times f_{\text{peak}} \times W \times t_{\text{policy}}\,.$$

This yields a *slight upper bound* (since $t_{\text{policy}} \geq t_{\text{actor}}$); spot checks in our regime found the gap within $\sim$3%.

From per-step to cumulative FLOPs. We compute $\text{FLOPs}_{\text{update}}$ per step from MFU and t_{policy}, then sum over steps:

$$\text{FLOPs}_{1:T} = \sum_{t=1}^{T} \text{MFU}_t\; f_{\text{peak}}\; W\; t_{\text{policy},t}\,.$$

These cumulative totals back the FLOPs–accuracy curves in Sec. 3.2.

Scope: what is counted and what is not. Our accounting *includes only* the parameter-update compute (forward + backward). It *excludes* (i) the rollout engine's generation compute and (ii) the *reference log-prob* pass (both of which VERL does not report MFU/FLOPs for). Under our settings (long responses, multi-sample trajectories), rollout consists of many forward passes, while the update consists of forward+backward over similar tokens; thus their compute is typically of the same *order of magnitude*, but exact ratios depend on response length, batching, and n (number of sampled trajectories). A precise FLOPs tally for rollout and reference log-prob computation is left to future work.

C Case Studies

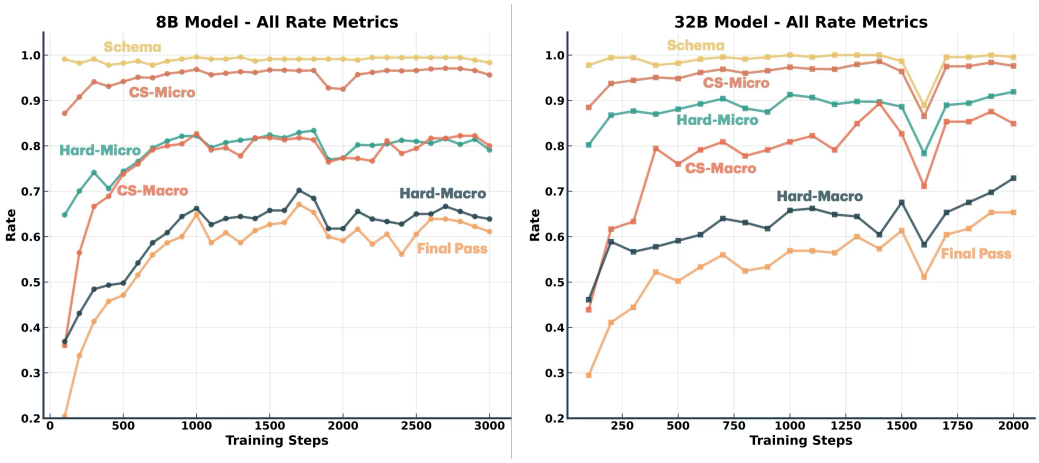

Figure A.1: Progression of six sub rewards for 8B and 32B Planner-R1 during training

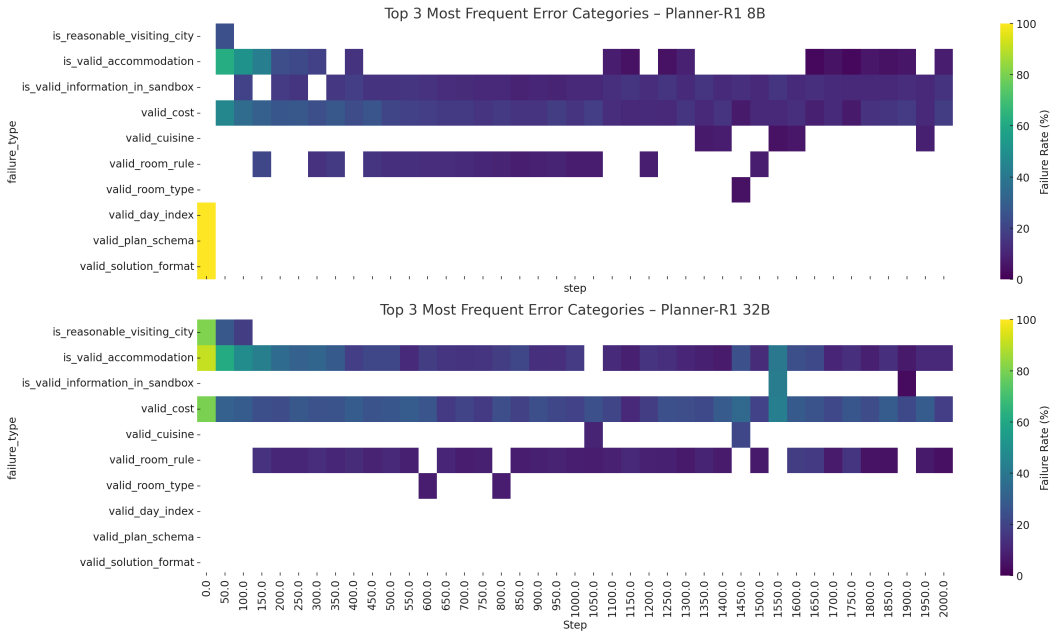

Figure A.2: Top 3 Most Frequent Error Categories for the Planner-R1 models. The upper heatmap shows the 8B model and the lower heatmap shows the 32B model. Both plots visualize, at each training step across five runs (up to 2000), the three most frequent failure categories and their relative rates. Rows are aligned so categories match across models; blank cells indicate that a category did not appear in the top three for that model at that step.

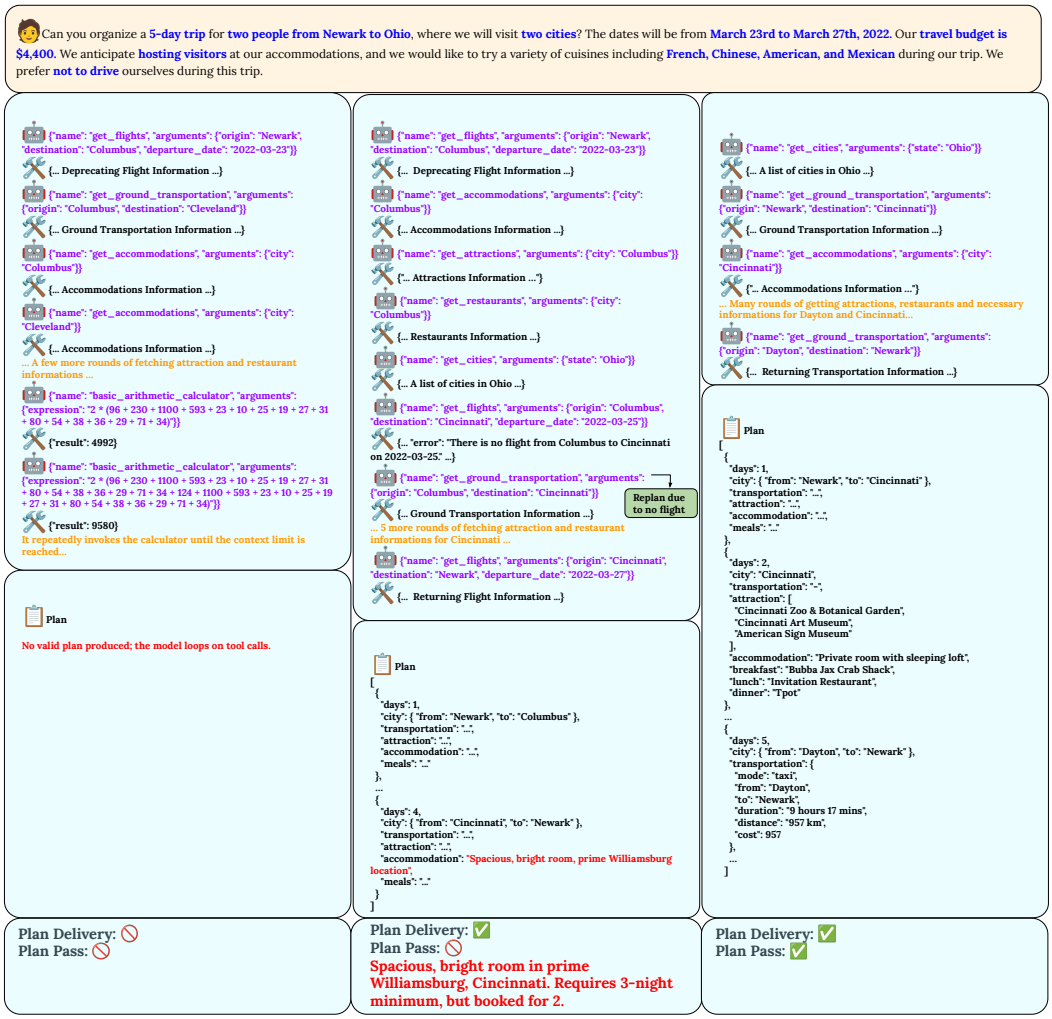

Figure A.3: Model tool-call trajectories across checkpoints. The base model (left) loops on repetitive tool calls once the context is saturated. After 100 training steps (middle), the model produces a coherent travel plan but fails to satisfy all constraints. By 500 steps with the 32B Planner-R1 checkpoint (right), the model successfully generates a valid plan that meets all requirements.

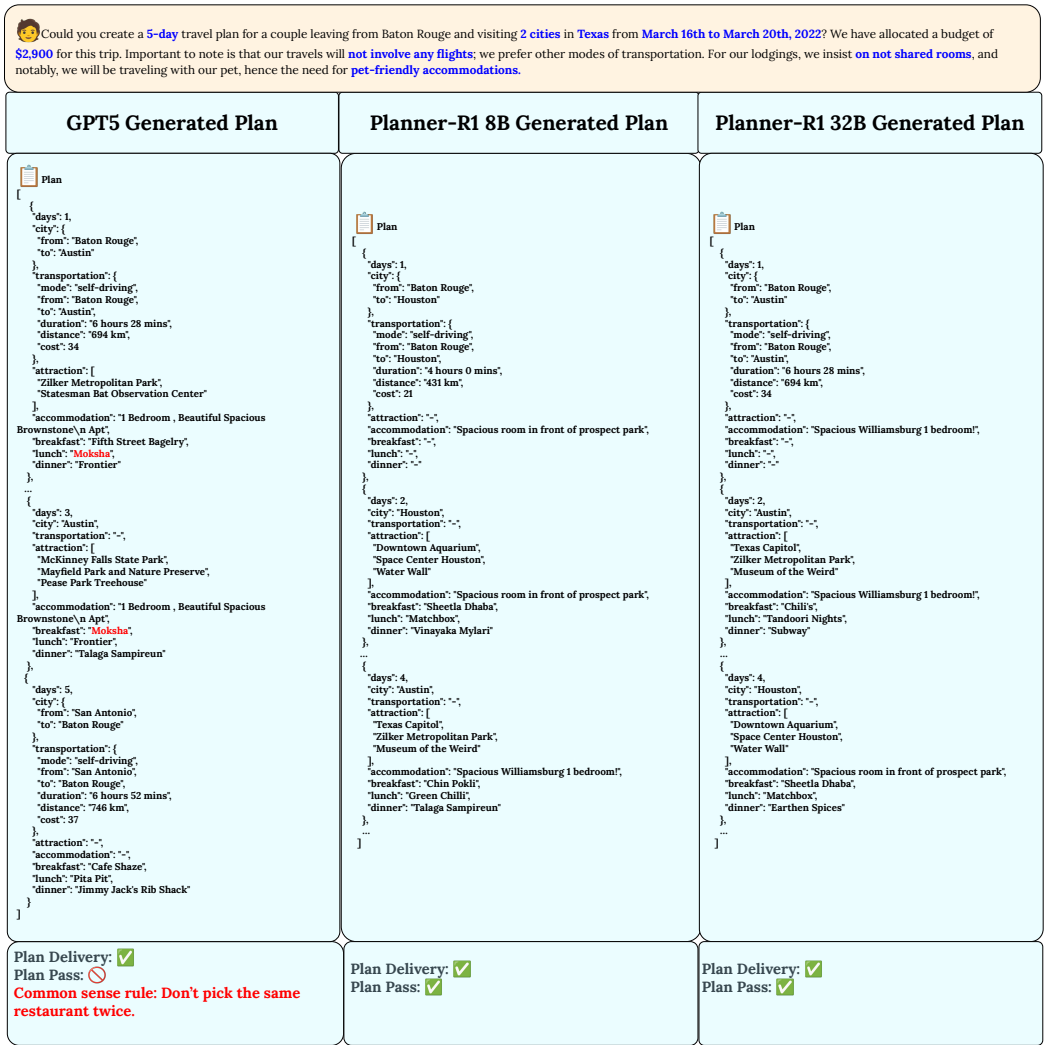

Figure A.4: The GPT-5 model (left) failed to avoid selecting the same restaurant twice, thus violating the common-sense rule. In contrast, the Planner-R1 8B model (middle) and Planner-R1 32B model (right) both generated plans that satisfied all requirements.

I need assistance in crafting a travel plan starting in Fort Lauderdale and covering **3 cities in Georgia**. The trip, designed for **2 people**, will span from **March 24th to March 30th**, 2022. Our budget is **$8,000**. Regarding accommodations, we require rooms that are not shared and should **accommodate children under 10**. As for dining options, we have diverse tastes, including **Indian, American, Chinese, and Mediterranean cuisines**.

GPT5 Generated Plan


```
  },
  "transportation": {
   "mode": "flight",
   "from": "Fort Lauderdale",
   "to": "Atlanta",
   "duration": "1 hours 40 minutes",
   "distance": "581 miles",
   "cost": 136,
   "flight_number": "F3543994",
   "departure_time": "09:35",
   "arrival_time": "11:15"
  },
  "attraction": [
   "World of Coca-Cola",
   "Centennial Olympic Park",
   "SkyView Atlanta"
  ],
  "accommodation": "Charming Carroll Gardens 2 BR",
  "breakfast": "-",
  "lunch": "Chef Style",
  "dinner": "Sethi's Restaurant & Barbeque"
 },
 {
  "days": 2,
  "city": "Atlanta",
  "transportation": "-",
  "attraction": [
   "Georgia Aquarium",
   "Atlanta Botanical Garden",
   "Piedmont Park",
   "High Museum of Art"
  ],
  "accommodation": "Charming Carroll Gardens 2 BR",
  "breakfast": "Daawat-e-Kashmir",
  "lunch": "Asian Bistro",
  "dinner": "Sam and Scrooge"
 },
 ...
 {
  "days": 5,
  "city": {
   "from": "Savannah",
   "to": "Augusta"
  },
  "transportation": {
   "mode": "self-driving",
   "from": "Savannah",
   "to": "Augusta",
   "duration": "2 hours 28 mins",
   "distance": "195 km",
   "cost": 9
  },
  "attraction": [
   "Augusta Riverwalk",
   "Augusta Museum of History",
   "Morris Museum of Art"
  ],
  "accommodation": "Planta Baja Studio",
  "breakfast": "New Raj Kachori Bhandar",
  "lunch": "Karari Kurry",
  "dinner": "Just Kababs"
 },
 {
  "days": 6,
  "city": {
   "from": "Augusta",
   "to": "Atlanta"
  },
  "transportation": {
   "mode": "self-driving",
   "from": "Augusta",
   "to": "Atlanta",
   "duration": "2 hours 13 mins",
   "distance": "233 km",
   "cost": 11
  },
  "attraction": [
   "Atlanta History Center",
   "Fox Theatre",
   "Krog Street Tunnel"
  ],
  "accommodation": "Charming Carroll Gardens 2 BR",
  "breakfast": "Haldiram's",
  "lunch": "Chaina Ram Sindhi Confectioners",
  "dinner": "Barkat"
 },
 {
  "days": 7,
  "city": {
   "from": "Atlanta",
   "to": "Fort Lauderdale"
  },
  "transportation": {
   "mode": "flight",
   "from": "Atlanta",
   "to": "Fort Lauderdale",
   "duration": "1 hours 38 minutes",
   "distance": "581 miles",
   "cost": 116,
   "flight_number": "F3963281",
   "departure_time": "17:01",
   "arrival_time": "18:39"
  },
  "attraction": "-",
  "accommodation": "-",
  "breakfast": "Baba Au Rhum",
  "lunch": "Nawaab",
  "dinner": "-"
 }
]
```


Plan Delivery: ✅
Plan Pass: 🚫
Common sense rule: City Atlanta is visited multiple times.

Planner-R1 8B Generated Plan


```
Plan
[
 {
  "days": 1,
  "city": {
   "from": "Fort Lauderdale",
   "to": "Atlanta"
  },
  "transportation": {
   "mode": "self-driving",
   "from": "Fort Lauderdale",
   "to": "Atlanta",
   "duration": "9 hours 5 mins",
   "distance": "1,031 km",
   "cost": 51
  },
  "attraction": "-",
  "accommodation": "Spacious private room close St. Barnabas Hospital",
  "breakfast": "-",
  "lunch": "-",
  "dinner": "-"
 },
 {
  "days": 2,
  "city": "Atlanta",
  "transportation": "-",
  "attraction": [
   "Atlanta Botanical Garden",
   "World of Coca-Cola",
   "Georgia Aquarium"
  ],
  "accommodation": "Spacious private room close St. Barnabas Hospital",
  "breakfast": "Pizza Central",
  "lunch": "Daawat-e-Kashmir",
  "dinner": "Chaina Ram Sindhi Confectioners"
 },
 ...
 {
  "days": 4,
  "city": "Savannah",
  "transportation": "-",
  "attraction": [
   "Forsyth Park",
   "Mercer-Williams House Museum",
   "Savannah Historic District"
  ],
  "accommodation": "Family and Friendly Room",
  "breakfast": "Sr. Sol 1",
  "lunch": "Bosphorous Turkish Cuisine",
  "dinner": "The Mad Teapot/The Wishing Chair"
 },
 {
  "days": 5,
  "city": {
   "from": "Savannah",
   "to": "Augusta"
  },
  "transportation": {
   "mode": "self-driving",
   "from": "Savannah",
   "to": "Augusta",
   "duration": "2 hours 28 mins",
   "distance": "195 km",
   "cost": 9
  },
  "attraction": "-",
  "accommodation": "Planta Baja Studio",
  "breakfast": "-",
  "lunch": "-",
  "dinner": "-"
 },
 {
  "days": 6,
  "city": "Augusta",
  "transportation": "-",
  "attraction": [
   "Phinizy Swamp Nature Park",
   "Augusta Riverwalk",
   "Augusta Museum of History"
  ],
  "accommodation": "Planta Baja Studio",
  "breakfast": "Vinny Vanucchi's",
  "lunch": "Fish Tales Lakeside Grille",
  "dinner": "Karari Kurry"
 },
 {
  "days": 7,
  "city": {
   "from": "Augusta",
   "to": "Fort Lauderdale"
  },
  "transportation": {
   "mode": "self-driving",
   "from": "Augusta",
   "to": "Fort Lauderdale",
   "duration": "8 hours 41 mins",
   "distance": "938 km",
   "cost": 46
  },
  "attraction": "-",
  "accommodation": "-",
  "breakfast": "-",
  "lunch": "-",
  "dinner": "-"
 }
]
```


Plan Delivery: ✅
Plan Pass: ✅

Planner-R1 32B Generated Plan


```
Plan
[
 {
  "days": 1,
  "city": {
   "from": "Fort Lauderdale",
   "to": "Augusta"
  },
  "transportation": {
   "mode": "self-driving",
   "from": "Fort Lauderdale",
   "to": "Augusta",
   "duration": "8 hours 39 mins",
   "distance": "936 km",
   "cost": 46
  },
  "attraction": "-",
  "accommodation": "Planta Baja Studio",
  "breakfast": "-",
  "lunch": "-",
  "dinner": "-"
 },
 {
  "days": 2,
  "city": "Augusta",
  "transportation": "-",
  "attraction": [
   "Phinizy Swamp Nature Park",
   "Augusta Riverwalk",
   "Augusta Museum of History"
  ],
  "accommodation": "Planta Baja Studio",
  "breakfast": "Vinny Vanucchi's",
  "lunch": "The Golden Dragon",
  "dinner": "Karari Kurry"
 },
 ...
 {
  "days": 4,
  "city": "Savannah",
  "transportation": "-",
  "attraction": [
   "Forsyth Park",
   "Wormsloe State Historic Site",
   "Mercer-Williams House Museum"
  ],
  "accommodation": "Family and Friendly Room",
  "breakfast": "Manohar Dairy And Restaurant",
  "lunch": "Bosphorous Turkish Cuisine",
  "dinner": "Dhaba On Wheels"
 },
 {
  "days": 5,
  "city": {
   "from": "Savannah",
   "to": "Atlanta"
  },
  "transportation": {
   "mode": "self-driving",
   "from": "Savannah",
   "to": "Atlanta",
   "duration": "3 hours 40 mins",
   "distance": "399 km",
   "cost": 19
  },
  "attraction": "-",
  "accommodation": "Charming Carroll Gardens 2 BR",
  "breakfast": "-",
  "lunch": "-",
  "dinner": "-"
 },
 {
  "days": 6,
  "city": "Atlanta",
  "transportation": "-",
  "attraction": [
   "Atlanta Botanical Garden",
   "World of Coca-Cola",
   "Georgia Aquarium"
  ],
  "accommodation": "Charming Carroll Gardens 2 BR",
  "breakfast": "Saffron",
  "lunch": "Pizza Central",
  "dinner": "Daawat-e-Kashmir"
 },
 {
  "days": 7,
  "city": {
   "from": "Atlanta",
   "to": "Fort Lauderdale"
  },
  "transportation": {
   "mode": "self-driving",
   "from": "Atlanta",
   "to": "Fort Lauderdale",
   "duration": "9 hours 6 mins",
   "distance": "1,030 km",
   "cost": 51
  },
  "attraction": "-",
  "accommodation": "-",
  "breakfast": "-",
  "lunch": "-",
  "dinner": "-"
 }
]
```


Plan Delivery: ✅
Plan Pass: ✅

Figure A.5: The GPT-5 model (left) selected the same restaurant twice on different dates, whereas the Planner-R1 8B (middle) and Planner-R1 32B (right) models produced plans that satisfied all requirements.

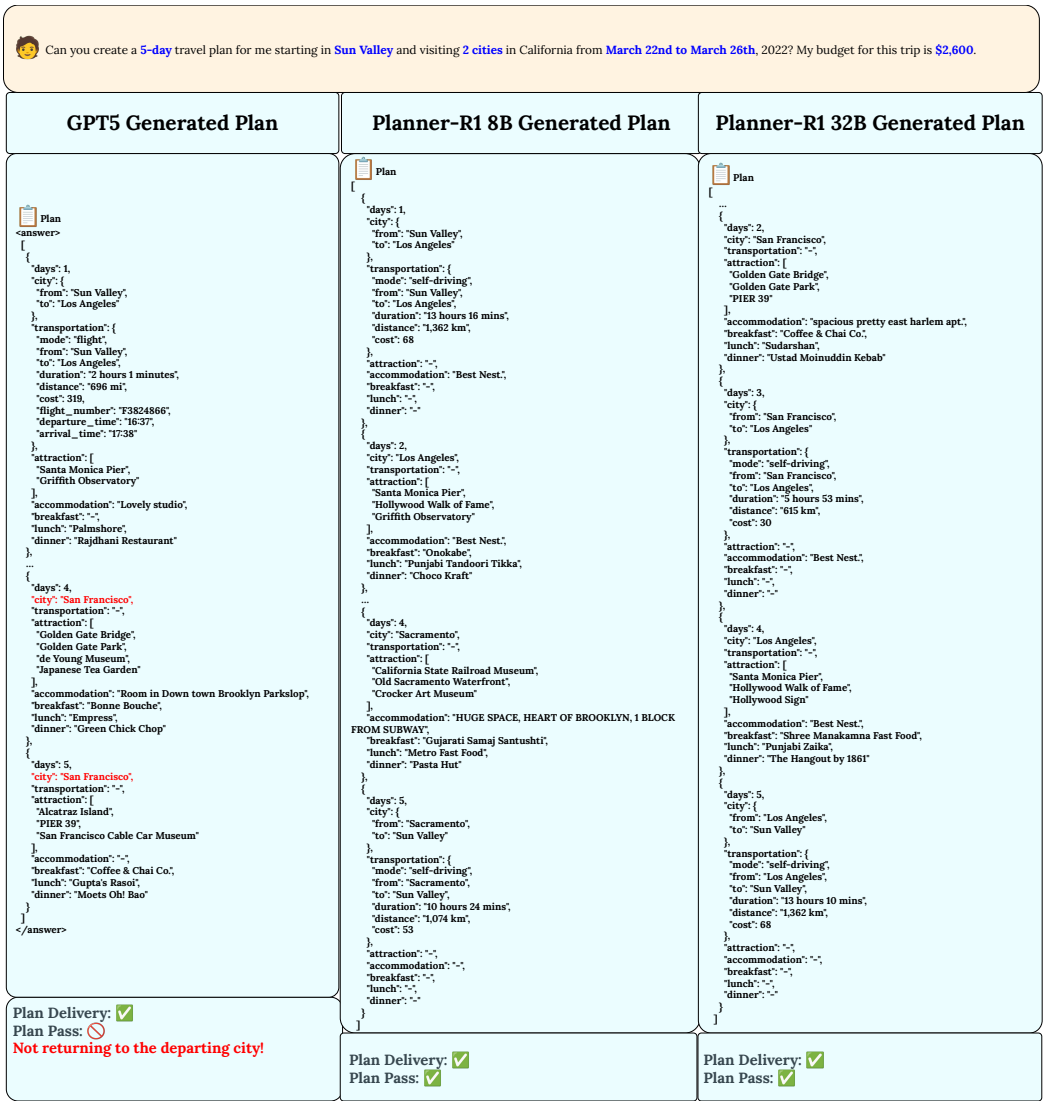

Figure A.6: The GPT-5 model (left) failed to return to the departing city, whereas the Planner-R1 8B (middle) and Planner-R1 32B (right) models produced plans that satisfied all requirements.

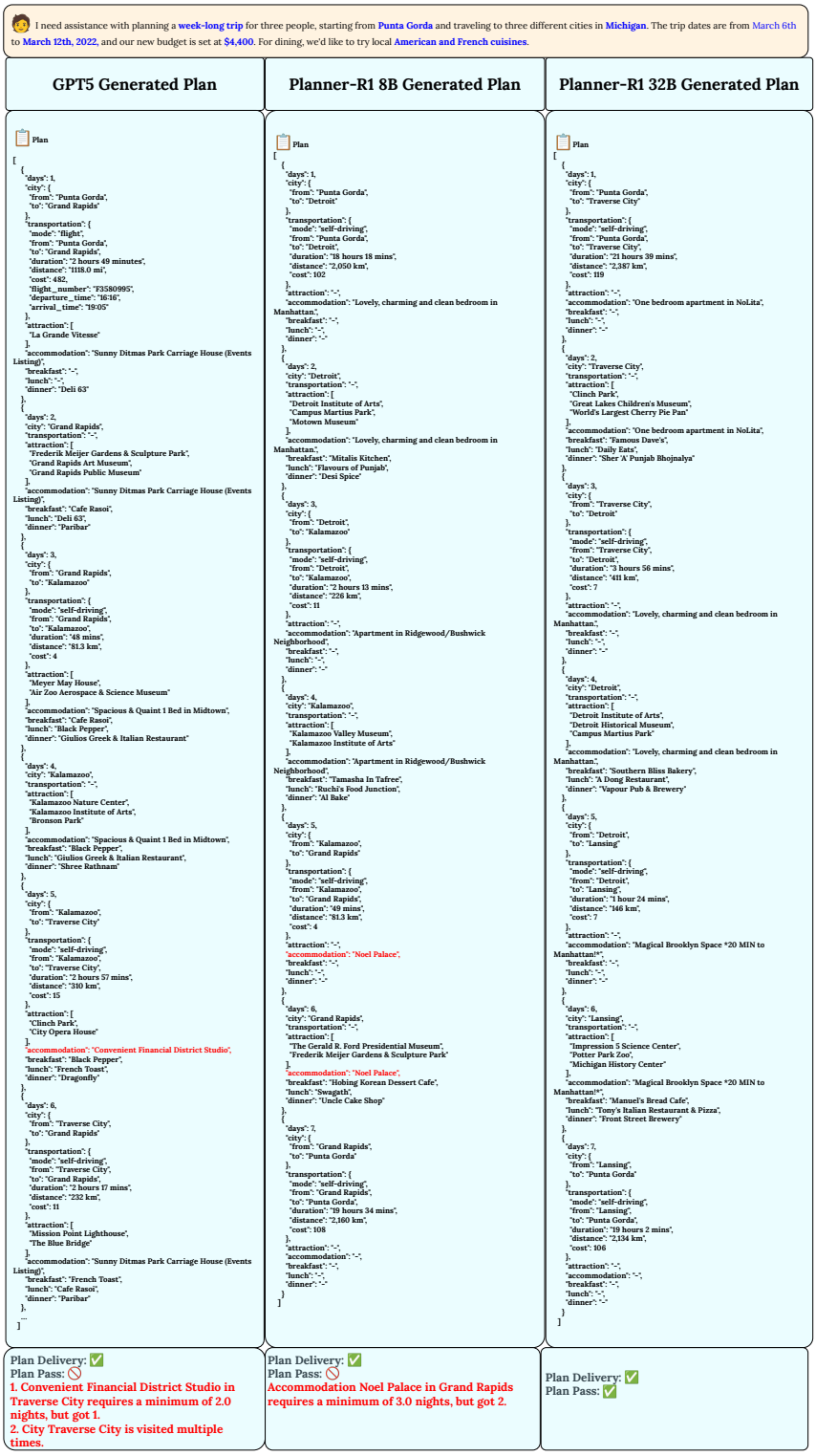

Figure A.7: The GPT-5 model (left) violated the hotel booking rule by reserving only one night instead of the required minimum of two, and also erred by visiting Traverse City multiple times, failing the common-sense requirement. The Planner-R1 8B model (middle) likewise failed the accommodation requirement, while only the Planner-R1 32B model (right) satisfied all requirements.

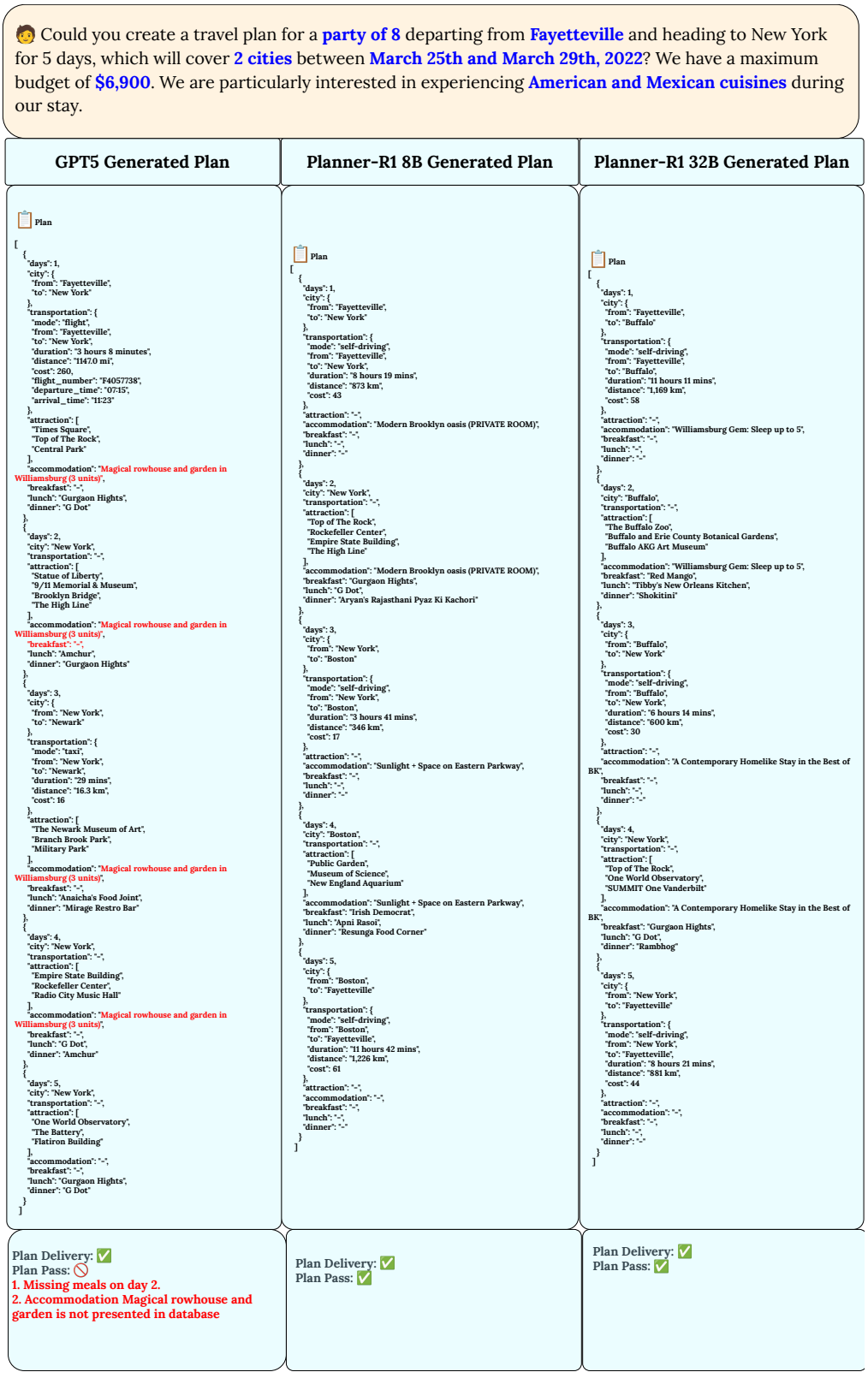

Figure A.8: In this query, the user plans a trip for a party of 8. The GPT-5 model (left) missed meals on Day 2 and hallucinated non-existent hotel names. The Planner-R1 8B model (middle) generated a plan that exceeded the $6,900 budget, while only the Planner-R1 32B model (right) satisfied all requirements.

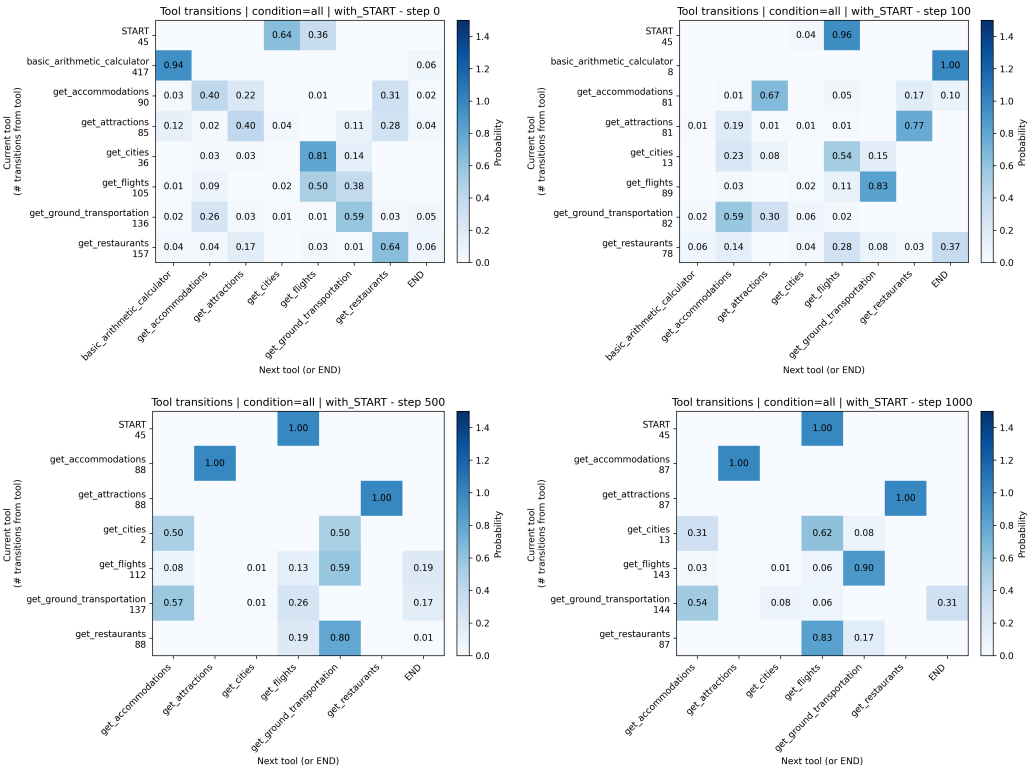

Figure A.9: Policy visualization for 8B model across 45 trajectories based on previous (y-axis) and next (x-axis) tool calls across various steps of learning: $\{0, 100, 500, 1000\}$. As learning progresses, the policy becomes more deterministic.

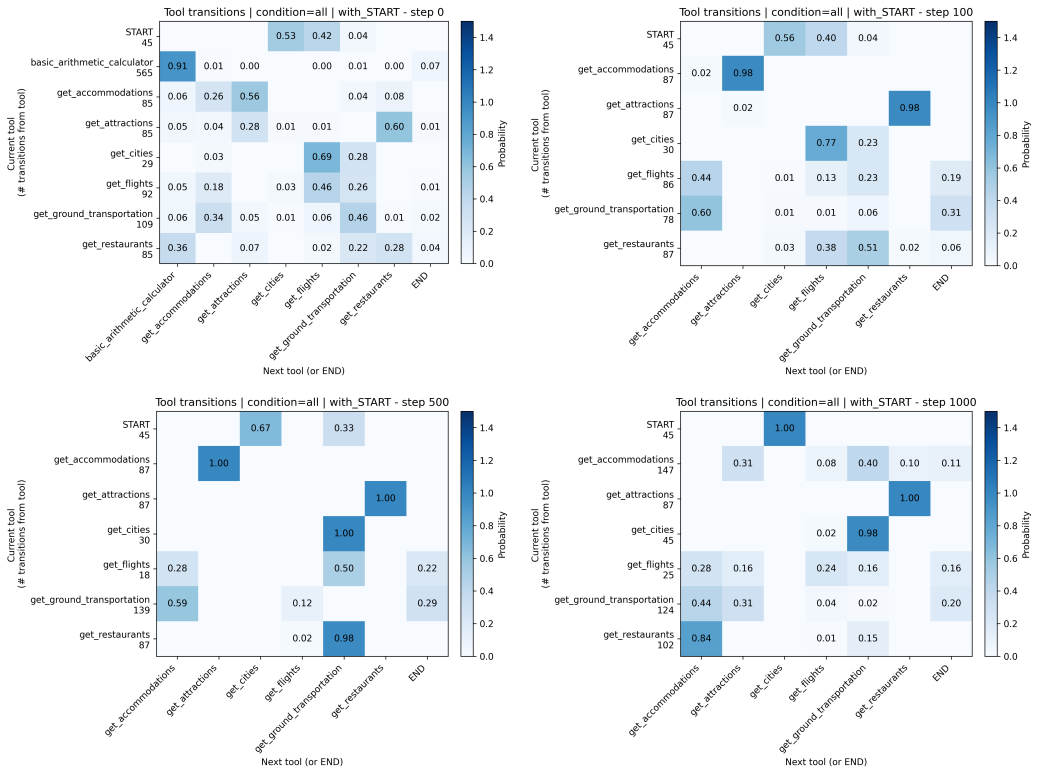

Figure A.10: Policy visualization 32B model across 45 trajectories based on previous (y-axis) and next (x-axis) tool calls across various steps of learning: $\{0, 100, 500, 1000\}$. As learning progresses, the policy becomes more deterministic.

Figure A.11: Tool call sequence behavior as 8B training progresses. The base model (leftmost) repeatedly invoked the calculator and restaurant tools until reaching the rollout cap (30 turns), exhibiting poor tool-use behavior as context grew. With longer training, the model developed more consistent and structured patterns for tool calls.

Figure A.12: Tool call sequence behavior as 32B training progresses. The base model (leftmost) repeatedly invoked the calculator until reaching the rollout cap (30 turns), exhibiting poor tool-use behavior as context grew, similar to the 8B model. With longer training, the model developed more consistent and structured patterns for tool calls. In particular, it learned to invoke get cities early to check available cities within states before searching for tickets and attractions. We also observed that the model made fewer get flights calls across queries, instead preferring to select more grounded transportation options.

LLM USAGE DISCLOSURE

We used large language models (LLMs) *only* as general-purpose writing assistants for surface-level language edits (grammar, phrasing, and clarity), LaTeX formatting suggestions (e.g., table/figure spacing, caption wording), and copyediting (e.g., consistent terminology, acronym expansion). LLMs did *not* contribute to research ideation, dataset or method design, experimental planning, implementation, analysis, or conclusions. All technical content, experiment setup, results, and interpretations were created and verified by the authors, who take full responsibility for the paper's substance and correctness.